JCI insight

Mature neutrophils suppress T cell immunity in ovarian cancer microenvironment

Kelly L. Singel, … , Emese Zsiros, Brahm H. Segal

JCI Insight. 2019. https://doi.org/10.1172/jci.insight.122311.

Research In-Press Preview **Immunology** **Oncology**

Epithelial ovarian cancer (EOC) often presents with metastases and ascites. Granulocytic myeloid-derived suppressor cells are an immature population that impairs anti-tumor immunity. Since suppressive granulocytes in the ascites of patients with newly diagnosed EOC were morphologically mature, we hypothesized that PMN were rendered suppressive in the tumor microenvironment. Circulating PMN from patients were not suppressive, but acquired a suppressor phenotype (defined as ≥ 1 $\log_{10}$ reduction of anti-CD3/CD28-stimulated T cell proliferation) after ascites supernatant exposure. Ascites supernatants (20/31) recapitulated the suppressor phenotype in PMN from healthy donors. T cell proliferation was restored with ascites supernatant removal and re-stimulation. PMN suppressors also inhibited T cell activation and cytokine production. PMN suppressors completely suppressed proliferation in naïve, central memory, and effector memory T cells, and in engineered tumor antigen-specific cytotoxic T lymphocytes, while antigen-specific cell lysis was unaffected. Inhibition of complement C3 activation and PMN effector functions, including CR3 signaling, protein synthesis, and vesicular trafficking, abrogated the PMN suppressor phenotype. Moreover, malignant effusions from patients with various metastatic cancers also induced the C3-dependent PMN suppressor phenotype. These results point to PMN impairing T cell expansion and activation in the tumor microenvironment and the potential for complement inhibition to abrogate this barrier to anti-tumor immunity.

Mature neutrophils suppress T cell immunity in ovarian cancer microenvironment

Kelly L. Singel[1]

Tiffany R. Emmons[1]

ANM Nazmul H. Khan[2]

Paul C. Mayor[3]

Shichen Shen[4]

Jerry T. Wong[5]

Kayla Morrell[6]

Kevin H. Eng[6]

Jaron Mark[3]

Richard B. Bankert[7]

Junko Matsuzaki[8]

Richard C. Koya[8]

Anna M. Blom[9]

Kenneth R. McLeish[10]

Jun Qu[4]

Sanjay Ram[11]

Kirsten B. Moysich[12]

Scott I. Abrams[1]

Kunle Odunsi[3,8]

Emese Zsiros[3,8]

Brahm H. Segal[1,2,13*]

Affiliations:

[1]Department of Immunology, Roswell Park Comprehensive Cancer Center, Buffalo, NY

[2]Department of Internal Medicine, Roswell Park Comprehensive Cancer Center, Buffalo, NY

[3]Department of Surgery, Division of Gynecologic Oncology, Roswell Park Comprehensive Cancer Center, Buffalo, NY

[4]New York State Center of Excellence Bioinformatics and Life Sciences, University at Buffalo, Buffalo, NY

[5]Department of Pathology and Laboratory Medicine, Roswell Park Comprehensive Cancer Center, Buffalo, NY

[6]Department of Biostatistics and Bioinformatics, Roswell Park Comprehensive Cancer Center, Buffalo, NY

[7]Department of Microbiology and Immunology, University at Buffalo Jacobs School of Medicine and Biomedical Sciences, Buffalo, NY

[8]Center for Immunotherapy, Roswell Park Comprehensive Cancer Center, Buffalo, NY

[9]Division of Medical Protein Chemistry, Department of Translational Medicine, Lund University, Malmö, Sweden

[10]Department of Medicine, University of Louisville School of Medicine, Louisville, KY

[11]Department of Medicine, University of Massachusetts Medical School, Worcester, MA

[12]Department of Cancer Prevention and Control, Roswell Park Comprehensive Cancer Center, Buffalo, NY

[13]Department of Medicine, Jacobs School of Medicine and Biomedical Sciences, University at Buffalo, Buffalo, NY

[*]Corresponding Author

Corresponding Author
Brahm H. Segal, MD, FACP, FIDSA
Chair, Department of Internal Medicine
Chief, Division of Infectious Diseases
Member, Dept. of Immunology
Roswell Park Comprehensive Cancer Center
Elm & Carlton Streets
Buffalo, NY 14263
716-845-5721 (voice)
brahm.segal@roswellpark.org (e-mail)

Running Title: Mature PMN suppress T cell responses in ovarian cancer

Key Words: Neutrophils, ovarian cancer, suppression, complement

Conflict of Interest Disclosure Statement
The authors have declared that no current conflict of interest exists. KLS, EZ, and BHS are co-inventors on a provisional patent application based on this manuscript.

Abstract

Epithelial ovarian cancer (EOC) often presents with metastases and ascites. Granulocytic myeloid-derived suppressor cells are an immature population that impairs anti-tumor immunity. Since suppressive granulocytes in the ascites of patients with newly diagnosed EOC were morphologically mature, we hypothesized that PMN were rendered suppressive in the tumor microenvironment (TME). Circulating PMN from patients were not suppressive, but acquired a suppressor phenotype (defined as ≥1 $\log_{10}$ reduction of anti-CD3/CD28-stimulated T cell proliferation) after ascites supernatant exposure. Ascites supernatants (20/31) recapitulated the suppressor phenotype in PMN from healthy donors. T cell proliferation was restored with ascites removal and re-stimulation. PMN suppressors also inhibited T cell activation and cytokine production. PMN suppressors completely suppressed proliferation in naïve, central memory, and effector memory T cells, and in engineered tumor antigen-specific cytotoxic T lymphocytes, while antigen-specific cell lysis was unaffected. Inhibition of complement C3 activation and PMN effector functions, including CR3 signaling, protein synthesis, and vesicular trafficking, abrogated the PMN suppressor phenotype. Moreover, malignant effusions from patients with various metastatic cancers also induced the C3-dependent PMN suppressor phenotype. These results point to PMN impairing T cell expansion and activation in the TME and the potential for complement inhibition to abrogate this barrier to anti-tumor immunity.

Introduction

Epithelial ovarian cancer (EOC) is typically diagnosed at advanced stages, presenting with peritoneal metastases and ascites accumulation. The tumor microenvironment (TME) of EOC is comprised of immunological niches that influence tumor progression and response to therapy (1). There is growing recognition for ascites as a distinct part of the EOC TME that facilitates seeding of serosal surfaces, mediates resistance to chemotherapy, and impairs anti-tumor immunity (2). Ascites contains specific tumor-associated lymphocyte populations that are being explored for cellular therapy (3), as well as immunosuppressive myeloid cells (4, 5) and exosomes (6) that are obstacles to anti-tumor immunity. Additional studies demonstrated distinct proteomic, glycosylation, and metabolic profiles in ascites that can affect tumor cell biology (7-9). The presence and volume of ascites at diagnosis of advanced EOC were associated with worse progression-free survival (PFS) and overall survival (OS) (10, 11). These findings point to both cellular and soluble constituents of ascites influencing metastasis, anti-tumor immune responses, and prognosis.

The critical role of T cell immunity in EOC was demonstrated by tumor-infiltrating $CD8^+$ T cells predicting better outcomes (12, 13), while increased accumulation of Treg was associated with worse outcomes (14). $CD8^+$ T cells that recognized NY-ESO-1, a tumor antigen, had impaired effector functions, but inhibiting LAG-3 and PD-1 signaling augmented proliferation and cytokine production (15). However, anti-PD-1 and anti-PD-L1 inhibitors have been largely ineffective in patients with relapsed/refractory EOC, with overall responses of 9-15% (16-18), raising the notion of other suppressive pathways in the TME as obstacles to immunotherapy.

Myeloid-derived suppressor cells (MDSC) are defined as immature myeloid cells that suppress T cell responses. They include myeloid progenitors and immature myeloid cells (19). Because MDSC markers overlap with other cell populations, phenotyping combined with demonstration of T cell suppression is optimal for identification of MDSC (20). Advanced cancer is associated with a myeloid bias characterized by increased frequencies of circulating

granulocyte-monocyte progenitors that are skewed towards differentiating into granulocytes (21). Tumor-derived factors, such as G-CSF, GM-CSF, and IL-6, drive this myeloid bias (22), and result in a circulating and tumor-infiltrating MDSC population that accelerates tumor progression by suppressing T cell responses and releasing factors that promote metastasis. Cui et al. (23) found that MDSC in EOC triggered acquisition of stem cell-like features in cancer cells and increased metastatic potential, and that myeloid cell ($CD33^+$) accumulation was associated with worse outcomes. Tumor-associated PMN (TAN) can be broadly divided into N1 (anti-tumorigenic) or N2 (suppressive and pro-tumorigenic) populations, with distinct transcriptional profiles and functional properties (24). These findings point to suppressive myeloid cells in the TME of EOC as barriers to anti-tumor immunity.

The concept of a myeloid bias can also apply to mature PMN. In patients with EOC, the pretreatment circulating PMN count (25) and the PMN-to-lymphocyte ratio (26) correlated with poor outcomes. Moreover, activated PMN can acquire a suppressive phenotype (27-29). There exists a gap in knowledge regarding the role of mature PMN as suppressor cells in the TME, as well as mechanisms for where and how PMN acquire a suppressive phenotype. The distinction between mature and immature suppressive granulocytes is mechanistically and therapeutically important. If circulating PMN are mature and acquire a suppressor phenotype within the TME, then therapeutic approaches should aim to disable their recruitment to the TME and target pathways driving suppression rather than to modulate myeloid programming in the marrow.

Since suppressive granulocytes in the ascites of patients with newly diagnosed EOC were morphologically mature, we hypothesized that mature, circulating PMN acquired a suppressor phenotype after recruitment to the TME. We recently observed that circulating PMN from healthy donors acquired a suppressor phenotype after exposure to ascites supernatants from patients with newly diagnosed advanced EOC (30). In the current study, we delineated mechanisms for this newly identified PMN suppressor phenotype. Inhibition of complement C3 activation and PMN effector functions, including CR3 signaling, protein synthesis, and vesicular

trafficking, abrogated the PMN suppressor phenotype. Together, these results point to mature PMN as the immunosuppressive granulocyte population in the EOC microenvironment and identify complement activation and other pathways for therapeutic modulation.

Results

Ovarian cancer ascites induce patient circulating PMN to become T cell suppressive.

Ascites from patients with newly diagnosed EOC contains monocytes/macrophages and granulocytes with variable immunosuppressive phenotypes (4, 5). Since MDSC are defined as immature, we compared the major populations of circulating and ascites WBC and their maturity based on standard cytologic criteria. In routine pre-operative CBC testing, patients with newly diagnosed EOC had normal circulating WBC numbers and differentials. Granulocytes were >99% mature segmented PMN, bands were <1%, and no immature granulocytes were observed **(Table 1)**. We found no difference in the proportions of circulating PMN ($CD45^+CD11b^+CD33^{mid}CD15^+CD14^{neg}DR^{neg}$) and monocytes ($CD45^+CD11b^+CD33^{hi}CD15^{neg}CD14^+DR^+$) between patients with high-grade serous ovarian cancer (HGSOC; accounts for majority of all cases) and female patients undergoing surgery for a benign adnexal mass (control blood) **(Figure 1A, Supplemental Figure 1)**. A hematopathologist (JTW) analyzed the cellular composition and morphology of granulocytes in Wright Giemsa-stained cytospins of ascites from patients with newly diagnosed metastatic HGSOC **(Figure 1B-C)**. The granulocytes had segmented nuclei with prominent filaments characteristic of mature PMN. No immature granulocytes were observed. The ascites PMN-to-lymphocyte ratio was 1.03 [95% CI 0.21-1.8, SEM 0.4] **(Figure 1D)**. These results demonstrate that the inflammatory microenvironment in ascites is distinct from blood, and circulating and ascites PMN are morphologically mature.

Because we previously observed that ascites granulocytes suppressed stimulated T cell proliferation (5), we evaluated whether circulating PMN from patients with advanced EOC were suppressive. We assessed the proliferation of anti-CD3/CD28-stimulated T cells from patients with newly diagnosed EOC (n=4) after incubation with media, autologous PMN, and/or ascites supernatants. The coculture PMN-to-lymphocyte ratio was 1:1, corresponding to the mean ratio observed in ascites. Addition of either PMN or ascites alone resulted in negligible reductions in

stimulated T cell proliferation **(Figure 1E and F)**. However, when added together, the interaction effect of PMN and ascites reduced T cell proliferation by a factor of 2.08 $\log_{10}$ [95% CI 1.26-2.90, *p=0.0002*] **(Figure 1F)**. These results establish that ascites induce mature PMN to acquire a suppressor phenotype, and are consistent with the hypothesis that mature, circulating PMN acquire this suppressor phenotype upon recruitment to the TME.

Ovarian cancer ascites induce circulating PMN from healthy donors to acquire the suppressor phenotype.

In patients with metastatic EOC, it is possible that tumor-derived factors could influence marrow and circulating granulocytes to render them more sensitive to the effects of ascites. We recently showed that ascites rendered PMN from healthy donors T cell suppressive (30). In the current study, we extended these results to include a larger number of EOC ascites and histology other than HGSOC (n=31; **Table 2**). PMN and T cells from a cohort of healthy donors were used for each experiment. Similar to patient PMN, ascites rendered PMN suppressive when cocultured with autologous T cells stimulated with anti-CD3/CD28 microbeads and soluble anti-CD3/CD28 Ab **(Figure 2A)**. Again, addition of PMN or ascites alone resulted in small biological effects (0.21 and 0.24 $\log_{10}$ reductions).

We stratified ascites (n=31) into three categories based on the induction of a PMN suppressor phenotype, where x equals a reduction in proliferation as compared to anti-CD3/CD28-stimulated T cells alone: suppressors ($x \geq 1$ $\log_{10}$), intermediate suppressors (0.5 $\log_{10} \leq x < 1$ $\log_{10}$), and non-suppressors ($x < 0.5$ $\log_{10}$) **(Figure 2B, Table 2)**. These results include ascites from n=22 HGSOC patients reported in our recent study (30). From this point on, we pre-selected ascites known to induce the PMN suppressor phenotype ($x \geq 1$ $\log_{10}$) in order to evaluate mechanisms for PMN-mediated suppression. Together, these findings show that mature PMN are the suppressive granulocytic population in EOC ascites, and are rendered suppressive by factors in the TME.

An effective anti-tumor response requires expansion and activation of tumor antigen-specific effector T cells in the TME. To determine whether the PMN suppressor phenotype affected central and effector memory T cells, we isolated naïve ($CD3^+CD45RA^+RO^{neg}CD62L^+$), central memory ($CD3^+CD45RA^{neg}RO^+CD62L^+$), and effector memory ($CD3^+CD45RA^{neg}RO^+CD62L^{neg}$) T cell populations from blood **(Supplemental Figure 2)**. All anti-CD3/CD28-stimulated T cell populations were suppressed by the PMN suppressor phenotype **(Figure 2C-E)**. Since the PMN suppressor phenotype had a similar effect on naïve, central memory, and effector memory T cells, we used unfractionated T cells in subsequent experiments. These findings showing that the PMN suppressor phenotype acts on the major circulating T cell populations, including effector memory T cells that drive anti-tumor immunity, support the importance of suppressive PMN as obstacles to anti-tumor immunity.

Suppressed T cells are viable and suppression is reversible.

We asked whether the observed reduction in stimulated T cell proliferation when cocultured with PMN and ascites was due to T cell apoptosis. The proportion of apoptotic stimulated T cells cocultured with media, ascites supernatants and/or PMN ranged from 17-27% **(Figure 2F)**. In addition, when T cells were cocultured with ascites and PMN, T cell proliferation was restored with ascites removal and anti-CD3/CD28 re-stimulation **(Figure 2G and H)**. Addition of recombinant IL-2 (rIL-2) to cocultures at 48h did not reverse T cell suppression **(Figure 2I)**. These results argue against T cell apoptosis as a mechanism for the PMN suppressor phenotype and show the potential for reversibility of T cell suppression.

Next, we carried out a series of experiments to identify the time frame of T cell suppression in relation to anti-CD3/CD28-stimulation and exposure to PMN and ascites. When T cells were anti-CD3/CD28-stimulated for 18h **(Supplemental Figure 3A)** or 1-6h **(Supplemental Figure 3B)** and then cocultured with ascites and PMN, T cell proliferation was unimpaired. However, when T cells were cocultured with ascites and PMN followed by addition

of anti-CD3/CD28-stimulation at various time points, suppression of T cell proliferation occurred when anti-CD3/CD28 was added within 1h of coculture, but was lost at 2h **(Supplemental Figure 3C)**. Surface expression of CD3 and CD28 on T cells after incubation with ascites and/or PMN was similar to T cells incubated with media **(Supplemental Figure 3D)**, indicating that the mechanism for T cell suppression is not due to loss of CD3 and CD28. These results show that the PMN suppressor phenotype requires PMN and ascites exposure early after T cell stimulation, is reversible, and raises the potential for therapeutically abrogating the suppressor phenotype.

PMN suppressor phenotype requires T cell contact and complement C3 activation.

We previously observed that ascites stimulated PMN degranulation and the generation of PMN extracellular traps (NETs) (30), raising the possibility that soluble products may be released into the coculture and mediate suppression of T cells. In the current study, when we exposed PMN to ascites for 6h and then added the PMN pellets or supernatants to anti-CD3/CD28-stimulated T cells, proliferation was unimpaired **(Supplemental Figure 3E)**. In addition, separation of PMN and T cells using a transwell system resulted in abrogation of suppression **(Figure 3A)**, suggesting that cell contact between PMN and T cells is required for suppression.

Complement receptor 3 (CR3; Mac-1; CD11b/CD18) mediates a critical step in PMN recruitment and cell-cell adhesion by binding to ICAM-1 on endothelial and T cells. Pretreating PMN with anti-CD11b Ab abrogated suppression, while pretreating T cells with anti-ICAM-1 Ab had no effect **(Figure 3B)**. Pretreating PMN or T cells with IgG1 as an isotype control had no effect. In humans, endotoxin (LPS) challenge or severe injury resulted in a subset of circulating PMN ($CD11c^{bright}CD62L^{dim}CD11b^{bright}CD16^{bright}$) that mediated T cell suppression through oxidant generation and CD11b (31). We observed that after 24h, PMN in media or ascites variably downregulated CD62L and CD16 expression, but there was no discernible population with increased CD16 expression as compared to baseline (data not shown), suggesting that the

PMN suppressor phenotype induced by ascites is distinct from circulating PMN suppressors induced by acute systemic inflammation. CR3 also binds iC3b, a cleavage product of C3 that acts as an opsonin and mediates intracellular signaling. Pretreating PMN with either C3b or iC3b prior to coculture resulted in abrogation of the suppressor phenotype, suggesting a desensitizing effect on PMN **(Figure 3C)**.

To determine if the factor in ascites inducing the PMN suppressor phenotype was complement-related, we first evaluated if it was a heat-labile protein(s) via heat-inactivation (HI-ASC; **Figure 3D**) and proteinase-K digestion (PK-ASC; **Supplemental Figure 4A**) of ascites supernatants prior to addition to cocultures. Both treatments completely abrogated T cell suppression. Since ascites exosomes can inhibit T cell responses (6), we determined whether the suppressive factor was membrane-associated or soluble. The ascites were ultracentrifuged to separate the membrane-rich (MR-ASC) and membrane-deplete (MD-ASC) fractions. The MR-ASC neither suppressed T cell proliferation alone nor in combination with PMN, while the MD-ASC rendered PMN suppressive **(Supplemental Figure 4B)**. These results show that soluble, heat-labile protein(s) in ascites are required for the PMN suppressor phenotype.

C3 plays a central role in the activation of the three complement pathways: classical, alternative, and lectin. Compstatins are a family of peptides that inhibit complement activation by binding to native C3 and interfering with convertase formation and C3 cleavage, and are being developed as therapeutics for complement-driven disorders (32, 33). To test the role of C3 activation in the PMN suppressor phenotype, we treated ascites with compstatin (CS-ASC; 250 μM; n=27) **(Figure 3E-G)** and Cp40 (Cp40-ASC; 20 μM; n=10) **(Figure 3H)** prior to coculture with PMN and T cells. Both completely abrogated the PMN suppressor phenotype, while scramble peptide (SCR-ASC) had no effect. The mean PMN viability (based on $PI^{neg}Annexin\text{-}V^{neg}$) after 24h exposure to Cp40-ASC (n=4) was 68 ± 8%, which was similar to untreated ascites (80 ± 8%) and SCR-ASC (80 ± 10%) *(p=ns)* (data not shown). PMN viability ranged between 41-47% at 54h under these conditions; these results do not support excess

PMN death as a mechanism for Cp40 abrogating the PMN suppressor phenotype. A concentration-titration study showed that 5 μM Cp40 was sufficient to fully abrogate the PMN suppressor phenotype **(Figure 3I)**.

To evaluate the role of downstream complement proteins in mediating the PMN suppressor phenotype, ascites were pretreated with Ab against C5 or with OmCI, a peptide C5 inhibitor derived from the saliva of *Ornithodoros moubata* (34, 35), prior to coculture. Inhibiting C5, with either antibody or peptide, had a partial abrogating effect on T cell suppression, as compared to Cp40 that fully abrogated the PMN suppressor phenotype **(Figure 3J)**. The membrane attack complex (MAC; C5b-C9) disrupts membranes of target cells leading to cell lysis. Ab against C7, a required component of MAC, had no effect on T cell suppression. These results show that functional CR3 and activation of C3 are required, C5 has an intermediate effect, and MAC is unlikely to be involved in the PMN suppressor phenotype.

Finally, we asked whether the PMN suppressor phenotype induced by EOC ascites would also occur following PMN exposure to other malignant effusions. We observed a similar PMN suppressor phenotype when PMN and anti-CD3/CD28-stimulated T cells were cocultured with malignant pleural and ascites supernatants from patients with a number of metastatic cancers (18/20 samples induced a PMN suppressor or intermediate suppressor phenotype). Using samples that met the suppressor definition **(Table 3)**, the PMN suppressor phenotype induced by malignant pleural and ascites was also abrogated by Cp40-treatment **(Figure 3K)**. These data demonstrate the generalizability of our findings regarding the C3-dependent induction of the PMN suppressor phenotype in malignant effusions.

Ascites activates multiple PMN effector pathways that mediate suppression.

We undertook a comprehensive analysis of the role of effector pathways in mediating the PMN suppressor phenotype. Since PMN degranulation can result in the release of suppressive products, including arginase-1 (28), we evaluated PMN surface expression for markers of fusion

of primary (CD63), secondary and tertiary (CD66b) granules, and secretory vesicles (CD35; complement receptor 1, CR1) after 30 and 60 min exposure to media, N-Formylmethionine-leucyl-phenylalanine (fMLF; positive control), ascites supernatants, or HI-ASC. CD63 surface expression was unaffected by ascites **(Figure 4A-B)**, and CD66b surface expression was no different between untreated ascites and HI-ASC **(Figure 4C-D)**. However, CD35/CR1 surface expression increased with ascites as compared to media, and decreased again with HI-ASC **(Figure 4E-F)**. These results suggest that ascites induce variable effects on fusion of PMN granules and secretory vesicles.

To assess the effect of endoplasmic reticulum (ER) transport on the PMN suppressor phenotype, we pretreated PMN with brefeldin-A and an ER export inhibitor, Exo1. Both agents abrogated the PMN suppressor phenotype **(Figure 4G)**. We further evaluated the role of exocytosis using fusion proteins containing the TAT cell permeability sequence and either the SNARE domain of syntaxin-4 or the N-terminal of SNAP23. SNARE decoys inhibit stimulated exocytosis of secretory vesicles and secondary and tertiary granules, but not primary granules, in PMN (36, 37). PMN pretreated with the SNARE decoys for SNAP23 and syntaxin-4 abrogated the PMN suppressor phenotype, while TAT fusion proteins with GST, a specificity control, had no effect **(Figure 4H)**. These results show that SNARE-dependent exocytosis is required for the PMN suppressor phenotype.

Activation with fMLF induced PMN to inhibit T cell responses through a mechanism requiring hydrogen peroxide generation (27). Therefore, we asked whether pretreatment of PMN prior to ascites exposure would desensitize PMN. We observed that activation with fMLF prevented induction of the PMN suppressor phenotype, indicative of heterologous desensitization **(Figure 4I).** In addition, PMN pretreated with thapsigargin (THG; inhibitor of Ca^{2+} mobilization) abrogated the PMN suppressor phenotype. To determine the role of PMN ROS in suppressing T cell proliferation, we evaluated the effect of the ROS scavenger, N-acetyl cysteine (NAC), and diphenyleneiodonium (DPI), a small molecule flavocytochrome inhibitor of

NADPH oxidase, the major source of PMN ROS generation. Addition of NAC to cocultures did not reverse suppression **(Supplemental Figure 5A)**, while pretreating PMN with DPI did abrogate the PMN suppressor phenotype **(Figure 4I)**. These results are conflicting regarding the role of ROS generation in the PMN suppressor phenotype; further studies using PMN from patients with chronic granulomatous disease (CGD), an inherited disorder of the phagocyte NADPH oxidase, will delineate the role of NADPH oxidase in the PMN suppressor function.

Release of arginase-1 from tertiary granules can also suppress T cells (28). Addition of L-arginine to the cocultures had no effect on T cell suppression **(Supplemental Figure 5A)**, arguing against arginase-1 mediating the PMN suppressor phenotype. We previously observed that ascites stimulated NET generation (30), and Lee et al. (38) recently demonstrated that NETs facilitated premetastatic niche formation in murine EOC. However, pretreatment of PMN with Cl-amidine, an inhibitor of protein arginine deiminase 4 required for NET generation, or addition of DNase I to the cocultures to degrade NETs, had no effect on the PMN suppressor phenotype **(Supplemental Figure 5A)**, suggesting that the mechanism is independent of NETs. Wong et al. (39) recently showed that IFN-gamma and TNF-alpha synergize to induce cyclooxygenase-2 (COX2) in the EOC TME, which in turn hyperactivates MDSC and leads to overexpression of the immunosuppressive enzyme, indoleamine-2,3-dioxygenase (IDO). We observed that addition of indomethacin, a non-selective COX inhibitor **(Supplemental Figure 5B)**, zileuton, an inhibitor of 5-lipoxygenase **(Supplemental Figure 5C)**, and 1-methyl-DL-tryptophan, an inhibitor of IDO1/2 **(Supplemental Figure 5D)**, to the cocultures had no effect on the PMN suppressor phenotype, indicating that the arachidonic acid pathway and IDO are likely not playing a role. Finally, high levels of TGF-beta are present in EOC ascites (40), and TGF-beta signaling can skew TAN to a suppressive N2 phenotype (24). We observed that anti-TGF-beta receptor 1 Ab did not abrogate the PMN suppressor phenotype **(Supplemental Figure 5E)**. Together, these results show that multiple PMN effector pathways are required for

mediation of the suppressor phenotype in mature PMN that are distinct from those associated with MDSC or N2 TAN.

Ascites induce robust protein synthesis in PMN that is required for the suppressor phenotype. We asked whether protein synthesis in PMN was required for the suppressor phenotype. Pretreating PMN with the protein synthesis inhibitors, puromycin and actinomycin D, resulted in variable abrogation of the suppressor phenotype **(Figure 5A)**. Based on these results, we explored the effect of ascites on protein production in PMN. We exposed PMN to media, ascites supernatants, or PK-ASC for 30- and 60-min, and subsequently underwent proteomics analysis. Unique protein groups (1,935) were quantified with ≥2 peptides per protein and <2% missing data rate on the protein level. Proteome patterns were similar at 30- and 60-min time points, and showed prominent discrepancies between PMN exposed to ascites versus PK-ASC **(Figure 5B)**. The PK-ASC-exposed PMN displayed a proteome pattern more similar to PMN exposed to media. Under the selected cutoff thresholds (>1.5-fold protein change, $p<0.05$) at 30- and 60-min, 630 and 638 proteins exhibited significant changes in the ascites groups, while only 160 and 195 proteins were significantly changed in the PK-ASC groups, respectively **(Figure 5C)**. Notably, 175 and 173 proteins were exclusively changed with 30- and 60-min ascites exposure, respectively. Gene ontology analysis of significant proteins showed enrichment of multiple classes of proteins with diverse biological functions in the ascites-exposed PMN **(Figure 5D)**. KEGG pathway analysis showed that the transcription factors, STAT3 and its target PU.1, were highly upregulated in PMN exposed to ascites, as compared to PMN exposed to media ($p=0.01$ and $p=0.002$, respectively). Ascites led to increased levels of several granular constituents, including myeloperoxidase *(p=0.005)*, neutrophil elastase *(p=0.0001)*, cathepsin G *(p=0.001)*, defensin 1 *(p=0.02)*, defensin 3 *(p=0.001)*, lysozyme C *(p=0.03)*, and MMP9 *(p=0.04)*. In addition, ascites exposure led to increased levels of multiple complement pathway and signaling components, including C1r *(p=0.003)*, C1q receptor *(p=0.01)*, C3 *(p<0.0001)*, C5 *(p<0.0001)*,

C9 *(p<0.0001)*, properdin *(p<0.001)*, factor B *(p<0.0001)*, and factor D *(p<0.0001)*, as well as CR1 (CD35, *p<0.0001*) and CR3 (CD18, *p=0.005*; CD11b, *p<0.0001*). Ascites also led to decreased levels of a smaller subset of proteins involved in protein folding, microtubule-based processes, and response to ROS, including $gp91^{phox}$ *(p=0.01)*, SOD *(p<0.0001)*, COX2 *(p<0.0001)*, NADPH-dependent carbonyl reductase *(p<0.0001)*, and promyelocytic leukemia protein *(PML, p=0.03)*. These results suggest that ascites induces synthesis of multiple classes of proteins in PMN, and protein synthesis is required for the PMN suppressor phenotype.

PMN suppressor phenotype inhibits stimulated naïve T cell activation without inducing exhaustion marker upregulation and without affecting antigen-specific CTL killing.

To further delineate the effects of the PMN suppressor phenotype on T cell immunity, we evaluated markers for T cell activation and exhaustion in cocultures. The proportion of CD62L-expressing T cells decreased after 24h of anti-CD3/CD28-stimulation as compared to baseline (characteristic of newly activated T cells), which was modulated by ascites or PMN alone, and inhibited in cocultures with ascites and PMN **(Figure 6A)**. The proportion of T cells expressing CD69 **(Figure 6B)**, CD40L **(Figure 6C)**, and CD107a **(Figure 6D)** increased with stimulation as compared to baseline (characteristic of newly activated T cells); in each case, upregulation was inhibited in cocultures with ascites and PMN. In addition, anti-CD3/CD28-stimulation upregulated the expression of exhaustion markers PD-1, LAG-3, and CTLA-4 on T cells **(Figure 6E-J)**. Coculture with ascites or PMN alone had more variable effects, while the combination of ascites and PMN prevented anti-CD3/CD28-stimulated upregulation of PD-1, LAG-3, and CTLA-4. Finally, while Cp40-ASC abrogated the PMN suppressor phenotype and enabled robust anti-CD3/CD28-stimulated T cell proliferation, Cp40-ASC did not result in upregulation of PD-1 or LAG-3 on T cells **(Figure 6K-L)**, while CTLA-4 expression was upregulated relative to unstimulated T cells **(Figure 6M)**.

Next, we evaluated the transcriptional control of $CD8^+$ effector differentiation, as measured by the upregulation of T-bet and Eomes (41). T-bet expression is associated with CTL differentiation while Eomes expression is associated with memory T cell differentiation. By gating on $CD3^+CD8^+CCR7^{neg}$ T cells **(Supplemental Figure 6A)**, anti-CD3/CD28-stimulation increased the proportion of $Eomes^+T\text{-}bet^{hi}$ T cells by 24h, as compared to unstimulated, and this increase contracted by 96h **(Supplemental Figure 6B-E)**. T cells cocultured with ascites and PMN phenocopied the $Eomes^+T\text{-}bet^{lo}$ signature of unstimulated cells **(Supplemental Figure 6F-G)**, indicating that the PMN suppressor phenotype inhibits differentiation into $CD8^+$ effector T cells. Ascites and/or PMN reduced the proportion of anti-CD3/CD28-stimulated $CD8^+$ T cells expressing IFN-gamma **(Figure 6N)**. In addition, ascites or PMN alone both reduced anti-CD3/CD28-stimulated production of IL-2 by T cells at 24 and 72h, while cocultures with ascites and PMN completely abrogated T cell IL-2 production **(Figure 6O-P)**. Together, these results show that the PMN suppressor phenotype inhibits T cell activation independently of upregulation of exhaustion marker expression, and has broad inhibitory effects on T cell activation, including the suppression of effector differentiation and cytokine responses.

Finally, we evaluated whether the PMN suppressor phenotype affected tumor cell lysis. NY-ESO-1-specific $CD8^+$ T cells from patients who received NY-ESO-1 vaccination were amplified *in vitro* and NYESO-$1_{157\text{-}165}$-specific $CD8^+$ T cells were isolated as described (42). Using NYESO-$1_{157\text{-}165}$-specific $CD8^+$ CTL and tumor cell (SK29) targets preloaded with NYESO-$1_{157\text{-}165}$ peptide, we observed that PMN and/or ascites had no effect on antigen-specific cytotoxicity **(Figure Q)**. Together, these results show that the PMN suppressor phenotype suppressed the expansion and activation of T cells without affecting CTL activity.

PMN suppressor phenotype inhibits the expansion of TCR-engineered CTL.

To further understand how the PMN suppressor phenotype may be a barrier to immunotherapy, we evaluated the effect of cocultures with ascites and PMN on CTL with engineered TCR that

411 recognize the tumor antigen, NY-ESO-1, and are in development for adoptive cellular therapy.
412 Engineered CTL are activated during the expansion process prior to use in cocultures,
413 accounting for the higher baseline proliferation observed in unstimulated cells and the modest
414 increase in proliferation observed in anti-CD3/CD28-stimulated cells **(Figure 7A)**. The PMN
415 suppressor phenotype inhibited stimulated proliferation of CTL below unstimulated levels, while
416 neither ascites nor PMN alone had an effect on proliferation. PK-ASC abrogated the PMN
417 suppressor phenotype, while MD-ASC had no effect, consistent with data in primary T cells. In
418 contrast to cocultures with primary T cells where rIL-2 did not reverse T cell suppression,
419 addition of rIL-2 to cocultures with engineered CTL at 48h completely restored proliferation,
420 suggesting that mechanisms for reversal of the PMN suppressor phenotype depends on
421 activation status of the T cells **(Figure 7B).** IFN-gamma expression was reduced to a similar
422 level after cocultures with PMN and/or ascites **(Figure 7C)**. These results point to the PMN
423 suppressor phenotype within the TME as a potential barrier to adoptive cellular therapy.

424 *Post-operative drainage fluid induces the PMN suppressor phenotype.*
425 Finally, we questioned if the PMN suppressor phenotype was specific to the TME or instead a
426 more general response to injury. We evaluated whether post-operative peritoneal fluid collected
427 from a surgical drain 1d after primary surgery for EOC would induce the PMN suppressor
428 phenotype. In contrast to ascites collected prior to surgery, which contained a mixed WBC
429 population, post-operative drainage fluid indicated a neutrophilic peritonitis **(Supplemental**
430 **Figure 7A-E)**. The numbers of cells in the post-operative drainage fluid were insufficient for
431 suppression studies. Therefore, we compared the capacity of paired ascites supernatants and
432 post-operative drainage supernatants to induce the PMN suppressor phenotype. The debulking
433 statuses of these patients were R0 (3/7), defined as no macroscopic residual tumor, or optimal
434 (4/7), defined by remaining disease 0.1-1 cm. Similar to ascites, post-operative drainage

435 supernatants were not suppressive alone, but induced PMN to suppress anti-CD3/CD28-
436 stimulated T cell proliferation **(Supplemental Figure 7F)**.

437 To further probe whether the PMN suppressor phenotype was specific to the TME, we
438 tested whether ascites supernatants from patients with cirrhosis and without cancer had the
439 ability to induce the PMN suppressor phenotype. We observed T cell suppression in 1/3
440 samples tested **(Supplemental Figure 7G)**. These findings support the notion that inflammation
441 and injury, whether resulting from the TME or other pathologic conditions, can induce the PMN
442 suppressor phenotype.

Discussion

Our results show that in patients with newly diagnosed advanced EOC, circulating PMN are not intrinsically suppressive, but acquire a suppressor phenotype once recruited to the TME. Ascites supernatants induced PMN to suppress stimulated T cell proliferation, activation, and cytokine responses, but did not affect CTL activity. These findings suggest that while the PMN suppressor phenotype will not affect the CTL activity of effector T cells, the phenotype will prevent the expansion of these CTL in the TME. The PMN suppressor phenotype inhibited T cell proliferation in stimulated naïve, central memory, and effector memory T cells, as well as in CTL with engineered TCR. Mature PMN fully recapitulated the suppressor phenotype attributed to granulocytic MDSC and N2 TAN. Although the distinction between granulocytic MDSC and N2 TAN is debated (19), the common feature is a circulating population of suppressor granulocytes (20, 43), while the PMN suppressor phenotype that we identified is acquired in the TME and dependent on several PMN effector functions. In addition, targeting TGF-beta signaling did not abrogate the phenotype, suggesting that this newly identified PMN suppressor phenotype is distinct from TGF-beta-driven N2 polarization. Moreover, malignant effusions from patients with various metastatic cancers also induced the C3-dependent PMN suppressor phenotype, supporting the generalizability of these findings. Together, these results point to mature PMN impairing T cell expansion and activation in the TME and identify a number of therapeutic targets to abrogate this barrier to anti-tumor immunity. Of the pathways driving the PMN suppressor phenotype, complement activation and signaling are likely to be the most promising therapeutic targets given the availability of approved and investigational inhibitors of complement components.

The role of complement activation in cancer is complex (44), and includes both pathways that can limit or worsen tumor growth. Complement can kill tumor cells through complement-dependent cytotoxicity, which is an important mechanism for tumor killing by monoclonal Ab. C3d enhanced anti-tumor immunity by increasing tumor infiltrating $CD8^+$ T cells,

depleting Tregs, and suppressing PD-1 expression on T cells (45). In addition, complement activation in tumor vasculature facilitated T cell homing and control of tumor in adoptive cellular therapy (46). However, tumor cells can secrete complement proteins that stimulate tumor growth and epithelial mesenchymal transition (47, 48). Complement activation can also promote platelet-granulocyte aggregation, thrombosis, and NETosis (49, 50). CR3 signaling was associated with suppression of NK cell function and increased growth of syngeneic melanoma (51). The C5aR1 peptide antagonist, PMX-53, improved the efficacy of Paclitaxel chemotherapy and was associated with the increased accumulation and cytotoxic function of $CD8^+$ effector memory T cells (52). In additional studies, the combination of C5a and anti-PD-1 blockade reduced tumor growth and metastasis (53). Most relevant to EOC, genetic and pharmacologic inhibition of complement blocked tumor growth through pathways dependent on VEGF and neovascularization in transgenic mice that develop EOC (54). Our results using human samples add to this body of literature by demonstrating a C3-dependent PMN suppressor phenotype induced by malignant effusions, and further support the concept of targeting complement to enhance immunotherapy.

A strength of our study was the use of ascites from patients, rather than tumor-conditioned media or tumor-bearing mice. Though the majority of ascites induced the PMN suppressor phenotype (≥ 1 $\log_{10}$ reduction of anti-CD3/CD28-stimulated T cell proliferation), this was not a universal finding. Our results point to soluble, heat-labile protein(s), specifically complement, in ascites inducing the PMN suppressor phenotype. Future studies involving fractionation and proteomics analysis of suppressor and non-suppressor ascites may delineate multiple proteins required for rendering PMN suppressive. A limitation of our study is that the small number of patients precluded an analysis of whether PMN accumulation in ascites or the capacity of ascites to induce the PMN suppressor phenotype correlated with outcomes.

PMN are easily activated when separated from whole blood. Erythrocyte sialoglycoproteins suppress PMN activation, and erythrocyte removal during purification can

release this inhibitory function (55). Negorev et al. (56) reported that PMN contaminated PBMC fractions after density gradient centrifugation methods used to isolate granulocytic MDSC, and may artefactually suppress T cell proliferation in certain cellular assays, including those that use microbeads for stimulation. We observed negligible to no effect of PMN alone in T cell suppression studies, while PMN combined with ascites supernatants resulted in dramatic suppression of T cell proliferation, frequently to unstimulated levels. The effect was observed with both anti-CD3/CD28 microbeads and soluble anti-CD3/CD28 Ab. Finally, we used a high standard for defining suppression as ≥ 1 $\log_{10}$ reduction in anti-CD3/CD28-stimulated T cell proliferation that was well above any background effects observed with PMN alone.

PMN can have considerable heterogeneity and plasticity, with the potential to enhance or suppress anti-tumor immunity (43, 57). Coffelt et al. (58) showed that PMN suppressed CTL responses, and depletion of IL-17 or G-CSF abrogated the T cell suppressive phenotype in a mammary tumor model. PMN have also enhanced mammary tumor metastasis to lungs (59). Targeting CXCR2, which mediates PMN recruitment, suppressed tumorigenesis and metastasis in mice (60), and dual targeting of CXCR2 and CCR2 enhanced responses to chemotherapy (61). Activated PMN can also kill tumor cells (62). Eruslanov et al. (63) showed that TAN from early stage lung cancer enhanced T cell responses. By contrast, our results show that PMN acquired a suppressor phenotype once exposed to the TME. Thus, the programming of PMN to a pro- or anti-tumorigenic phenotype depends on cues within the TME that include tumor-derived factors and products of inflammation and injury.

In response to infection, activation of CR3 on PMN leads to a signaling cascade that results in the phagocytosis of extracellular pathogens and downstream activation of Syk (64) and NADPH oxidase required for clearance of pathogens (65, 66). In the TME, our results point to several PMN effector functions that normally function to eradicate pathogens becoming barriers to anti-tumor immunity by impairing the activation and expansion of T cells. There is precedent for MDSC limiting T cell activation through ROS cross-signaling and inhibition of TCR

signaling (67, 68). Studies are in progress to test whether NADPH oxidase-deficient PMN from CGD patients acquire a suppressor phenotype following ascites exposure. While a mechanism for PMN-mediated suppression is induction of $CD8^+$ T cell apoptosis (69), we did not observe a clear effect of PMN and/or ascites on T cell viability. In addition, T cell proliferation was restored with ascites removal and re-stimulation highlighting the potential for therapeutically reversing the quiescent phenotype of T cells. Gao et al. (70) described apoptotic PMN that suppress T cells in a cell contact and ROS-dependent mechanism. While C3 inhibition with Cp40 fully abrogated the PMN suppressor phenotype, it did not significantly affect PMN viability. However, this finding doesn't exclude the potential for apoptosis/anti-apoptosis pathways influencing the PMN suppressor phenotype.

Ascites induced the synthesis of a strikingly large number of proteins mediating multiple effector functions in PMN, which was required for the suppressor phenotype. Grassi et al. (71) identified stage-specific transcriptome and epigenetic changes in PMN maturation in which granular constituents are produced during granulopoiesis in the marrow, and the signaling components that activate them are transcribed at later stages in circulation. Mature PMN maintain activated levels of PU.1 and can synthesize new proteins through a number of pathways (72-74). A limitation of this proteomics analysis is that we cannot discriminate between newly synthesized proteins versus intracellular transport of proteins from the ascites. Future studies will delineate the transcriptional and epigenetic changes in PMN induced by ascites exposure and the relationship with proteomic changes.

Finally, we observed that post-operative drainage fluid induced the PMN suppressor phenotype similar to paired pre-operative ascites. This finding was observed in patients with R0 and optimal debulking surgeries. Since primary surgery for advanced EOC is non-curative, post-surgical immunosuppression is likely to be clinically relevant. We observed that the new microenvironment was characterized by an early neutrophilic peritonitis, which others have reported should be followed by wound healing responses, including the accumulation of

immunosuppressive cells that can promote growth of residual tumor (75). The concept of the pro-tumorigenic effect of surgery is indirectly supported by short delays in adjuvant chemotherapy after primary surgery for EOC that correlate with shorter PFS and OS (76, 77). Our finding that post-operative drainage fluid induced the PMN suppressor phenotype is consistent with the findings that acute inflammatory conditions unrelated to cancer (e.g., LPS challenge, severe injury, and sepsis) can induce an expansion of suppressive granulocytes in humans (31, 78). These findings suggest that the expansion of suppressive PMN, both immature and mature, can occur in response to multiple insults and through distinct signaling pathways. Further studies are warranted to compare the transcriptional and proteomic profiles and functional characteristics of the PMN suppressor phenotype induced in the TME compared to other acute and chronic inflammatory conditions. The induction of suppressive PMN may be a strategy to limit tissue injury or avert autoimmunity by restraining T cell responses; while in the TME, these same pathways are predicted to impede anti-tumor immunity.

Methods

Patients and Specimens

Participants included healthy donors, control female patients with a benign adnexal mass undergoing resection surgery, and cancer patients with malignant effusions. Healthy donors (n=4) were Caucasian, aged 26-51, and equally divided between sexes. From 2015-2017, blood and ascites were collected from patients with newly diagnosed advanced (stage III or IV) ovarian cancer, as previously described (79). Blood was collected prior to primary surgery, and ascites were collected either by diagnostic paracentesis or in the operating room prior to surgery. Ascites were filtered through 300 μM filters and then centrifuged (500g, 10 min). Aliquots of supernatants were stored at -80°C until further use. When available, post-operative drainage fluid from an abdominal drainage tube was collected the day after primary surgery. Patients with early stage (I or II) or unstaged disease were excluded from the analysis. The medical records of these patients were retrospectively reviewed for demographics, tumor stage and grade, baseline serum CA125 levels, debulking status, and chemotherapy response. In 2018, malignant pleural effusions were collected by thoracentesis from patients with various metastatic cancers and processed following the same protocol.

Analysis of Immune Infiltrate in Peripheral Blood and Ascites

Peripheral blood was collected in EDTA-coated tubes (Vacutainer, BD Biosciences, San Jose, CA). Whole blood was washed with PBS and centrifuged (500g, 10 min). Cells from blood and ascites were analyzed by flow cytometry within 24h. Flow cytometry analysis was conducted on a Fortessa (Becton Dickinson, Franklin Lakes, NJ). Forward scatter versus side scatter gating was set to include all non-aggregated cells from at least 20,000 events collected per sample. Data were analyzed using WinList 9.0.

Isolation of PMN and T cells from Peripheral Blood

PMN and T cells were isolated from peripheral blood <1h post-collection using the MACSxpress Neutrophil Isolation Kit and the CD4, CD8, or Pan T cell Isolation Kits, respectively (Miltenyi Biotec, Inc, Auburn, CA, USA). The purity of PMN was >96% based on cytology and $CD45^+CD33^{mid}CD15^+CD66b^+$ (80); there was complete concordance between CD15 and CD66b expression. The purity of T cells was >97% based on $CD45^+CD3^+$, $CD45^+CD3^+CD4^+$, and $CD45^+CD3^+CD8^+$ expression.

Statistics

All statistical analyses were performed using the R 3.4.0 statistical computing language. A nominal significance threshold of 0.05 was used unless otherwise specified. Statistical testing utilized ANOVA to determine significance followed by a Tukey multiple comparisons post-test to determine which groups were significant. Pre-specified interactions were tested within the ANOVA framework. The multivariate analysis comprised FIGO stage, categorized as early (I, II, or IIIA/B) or late (IIIC or IV), histological grade, serum CA125 levels, debulking status (R0, defined as no macroscopic residual disease; optimal, defined by remaining disease 0.1-1 cm; and suboptimal, defined by remaining visible disease >1 cm), and platinum-sensitive versus refractory disease.

Study Approval

This study was approved by the Institutional Review Board (IRB) of Roswell Park Comprehensive Cancer Center (Roswell Park), Buffalo, NY, and was in compliance with federal and state requirements. All participants gave informed consent prior to inclusion in the study (protocols i215512 and i188310). All studies were conducted in compliance with the Declaration of Helsinki.

Author Contributions

All authors contributed extensively to the work presented in this paper. KLS and BHS developed the study and wrote the manuscript. KLS, TRE, ANHK, PCM, SS, JTW, JM, and JM designed

609 and performed experiments, and analyzed data. KM and KHE analyzed and described the
610 statistical models, and contributed to the manuscript. RCK, AB, and KRM provided reagents.
611 JTW, RBB, RCK, AB, KRM, SR, JQ, KBM, SIA, KO, EZ, and BHS provided technical support
612 and conceptual advice. All authors discussed the results and implications, and commented on
613 the manuscript at all stages.

614 *Acknowledgements*

615 This work was supported by Roswell Park Comprehensive Cancer Center grants NCI
616 P30CA016056, the Roswell Park-UPCI Ovarian Cancer SPORE P50CA159981 (KO),
617 5R01CA188900 (BHS and KBM), R01CA172105 (SIA), 5T32CA108456 (PCM and JM),
618 T32CA085183 (KLS), and K01LM012100 (KHE). The funders had no role in study design, data
619 collection and analysis, decision to publish, or preparation of the manuscript. We would like to
620 thank Drs. John D. Lambris (Department of Pathology and Laboratory Medicine, University of
621 Pennsylvania Perelman School of Medicine, Philadelphia, PA) and William M. Nauseef
622 (Department of Internal Medicine and Inflammation Program, Carver College of Medicine
623 University of Iowa, Iowa City, IA) for providing reagents and helpful discussions.

References

1. Jimenez-Sanchez A, Memon D, Pourpe S, Veeraraghavan H, Li Y, Vargas HA, et al. Heterogeneous Tumor-Immune Microenvironments among Differentially Growing Metastases in an Ovarian Cancer Patient. *Cell.* 2017;170(5):927-38 e20.
2. Worzfeld T, Pogge von Strandmann E, Huber M, Adhikary T, Wagner U, Reinartz S, et al. The Unique Molecular and Cellular Microenvironment of Ovarian Cancer. *Front Oncol.* 2017;7:24.
3. Idorn M, Olsen M, Halldorsdottir HR, Skadborg SK, Pedersen M, Hogdall C, et al. Improved migration of tumor ascites lymphocytes to ovarian cancer microenvironment by CXCR2 transduction. *Oncoimmunology.* 2018;7(4):e1412029.
4. Obermajer N, Muthuswamy R, Odunsi K, Edwards RP, and Kalinski P. PGE(2)-induced CXCL12 production and CXCR4 expression controls the accumulation of human MDSCs in ovarian cancer environment. *Cancer research.* 2011;71(24):7463-70.
5. Khan AN, Kolomeyevskaya N, Singel KL, Grimm MJ, Moysich KB, Daudi S, et al. Targeting myeloid cells in the tumor microenvironment enhances vaccine efficacy in murine epithelial ovarian cancer. *Oncotarget.* 2015;6(13):11310-26.
6. Shenoy GN, Loyall J, Maguire O, Iyer V, Kelleher RJ, Jr., Minderman H, et al. Exosomes Associated with Human Ovarian Tumors Harbor a Reversible Checkpoint of T-cell Responses. *Cancer immunology research.* 2018;6(2):236-47.
7. Shender VO, Pavlyukov MS, Ziganshin RH, Arapidi GP, Kovalchuk SI, Anikanov NA, et al. Proteome-metabolome profiling of ovarian cancer ascites reveals novel components involved in intercellular communication. *Mol Cell Proteomics.* 2014;13(12):3558-71.
8. Biskup K, Braicu EI, Sehouli J, Tauber R, and Blanchard V. The ascites N-glycome of epithelial ovarian cancer patients. *Journal of proteomics.* 2017;157:33-9.

9. Worzfeld T, Finkernagel F, Reinartz S, Konzer A, Adhikary T, Nist A, et al. Proteotranscriptomics Reveal Signaling Networks in the Ovarian Cancer Microenvironment. *Mol Cell Proteomics.* 2018;17(2):270-89.
10. Huang H, Li YJ, Lan CY, Huang QD, Feng YL, Huang YW, et al. Clinical significance of ascites in epithelial ovarian cancer. *Neoplasma.* 2013;60(5):546-52.
11. Szender JB, Emmons T, Belliotti S, Dickson D, Khan A, Morrell K, et al. Impact of ascites volume on clinical outcomes in ovarian cancer: A cohort study. *Gynecologic oncology.* 2017;146(3):491-7.
12. Zhang L, Conejo-Garcia JR, Katsaros D, Gimotty PA, Massobrio M, Regnani G, et al. Intratumoral T cells, recurrence, and survival in epithelial ovarian cancer. *The New England journal of medicine.* 2003;348(3):203-13.
13. Sato E, Olson SH, Ahn J, Bundy B, Nishikawa H, Qian F, et al. Intraepithelial CD8+ tumor-infiltrating lymphocytes and a high CD8+/regulatory T cell ratio are associated with favorable prognosis in ovarian cancer. *Proceedings of the National Academy of Sciences of the United States of America.* 2005;102(51):18538-43.
14. Curiel TJ, Coukos G, Zou L, Alvarez X, Cheng P, Mottram P, et al. Specific recruitment of regulatory T cells in ovarian carcinoma fosters immune privilege and predicts reduced survival. *Nature medicine.* 2004;10(9):942-9.
15. Matsuzaki J, Gnjatic S, Mhawech-Fauceglia P, Beck A, Miller A, Tsuji T, et al. Tumor-infiltrating NY-ESO-1-specific CD8+ T cells are negatively regulated by LAG-3 and PD-1 in human ovarian cancer. *Proceedings of the National Academy of Sciences of the United States of America.* 2010;107(17):7875-80.
16. Brahmer JR, Tykodi SS, Chow LQ, Hwu WJ, Topalian SL, Hwu P, et al. Safety and activity of anti-PD-L1 antibody in patients with advanced cancer. *The New England journal of medicine.* 2012;366(26):2455-65.

17. Hamanishi J, Mandai M, Ikeda T, Minami M, Kawaguchi A, Murayama T, et al. Safety and Antitumor Activity of Anti-PD-1 Antibody, Nivolumab, in Patients With Platinum-Resistant Ovarian Cancer. *J Clin Oncol.* 2015;33(34):4015-22.
18. Matulonis UA, Shapira-Frommer R, Santin A, Lisyanskaya AS, Pignata S, Vergote I, et al. Antitumor activity and safety of pembrolizumab in patients with advanced recurrent ovarian cancer: Interim results from the phase 2 KEYNOTE-100 study. *J Clin Oncol.* 2018(36):abstr 5511.
19. Veglia F, Perego M, and Gabrilovich D. Myeloid-derived suppressor cells coming of age. *Nature immunology.* 2018;19(2):108-19.
20. Bronte V, Brandau S, Chen SH, Colombo MP, Frey AB, Greten TF, et al. Recommendations for myeloid-derived suppressor cell nomenclature and characterization standards. *Nat Commun.* 2016;7:12150.
21. Wu WC, Sun HW, Chen HT, Liang J, Yu XJ, Wu C, et al. Circulating hematopoietic stem and progenitor cells are myeloid-biased in cancer patients. *Proceedings of the National Academy of Sciences of the United States of America.* 2014;111(11):4221-6.
22. Netherby CS, Messmer MN, Burkard-Mandel L, Colligan S, Miller A, Cortes Gomez E, et al. The Granulocyte Progenitor Stage Is a Key Target of IRF8-Mediated Regulation of Myeloid-Derived Suppressor Cell Production. *J Immunol.* 2017;198(10):4129-39.
23. Cui TX, Kryczek I, Zhao L, Zhao E, Kuick R, Roh MH, et al. Myeloid-derived suppressor cells enhance stemness of cancer cells by inducing microRNA101 and suppressing the corepressor CtBP2. *Immunity.* 2013;39(3):611-21.
24. Shaul ME, Levy L, Sun J, Mishalian I, Singhal S, Kapoor V, et al. Tumor-associated neutrophils display a distinct N1 profile following TGFbeta modulation: A transcriptomics analysis of pro- vs. antitumor TANs. *Oncoimmunology.* 2016;5(11):e1232221.
25. Banerjee S, Rustin G, Paul J, Williams C, Pledge S, Gabra H, et al. A multicenter, randomized trial of flat dosing versus intrapatient dose escalation of single-agent

carboplatin as first-line chemotherapy for advanced ovarian cancer: an SGCTG (SCOTROC 4) and ANZGOG study on behalf of GCIG. *Annals of oncology : official journal of the European Society for Medical Oncology / ESMO.* 2013;24(3):679-87.

26. Huang QT, Zhou L, Zeng WJ, Ma QQ, Wang W, Zhong M, et al. Prognostic Significance of Neutrophil-to-Lymphocyte Ratio in Ovarian Cancer: A Systematic Review and Meta-Analysis of Observational Studies. *Cellular physiology and biochemistry : international journal of experimental cellular physiology, biochemistry, and pharmacology.* 2017;41(6):2411-8.

27. Schmielau J, and Finn OJ. Activated granulocytes and granulocyte-derived hydrogen peroxide are the underlying mechanism of suppression of t-cell function in advanced cancer patients. *Cancer research.* 2001;61(12):4756-60.

28. Rotondo R, Bertolotto M, Barisione G, Astigiano S, Mandruzzato S, Ottonello L, et al. Exocytosis of azurophil and arginase 1-containing granules by activated polymorphonuclear neutrophils is required to inhibit T lymphocyte proliferation. *J Leukoc Biol.* 2011;89(5):721-7.

29. Tak T, Rygiel TP, Karnam G, Bastian OW, Boon L, Viveen M, et al. Neutrophil-mediated Suppression of Influenza-induced Pathology Requires CD11b/CD18 (MAC-1). *American journal of respiratory cell and molecular biology.* 2018;58(4):492-9.

30. Singel KL, Grzankowski KS, Khan A, Grimm MJ, D'Auria AC, Morrell K, et al. Mitochondrial DNA in the tumour microenvironment activates neutrophils and is associated with worse outcomes in patients with advanced epithelial ovarian cancer. *British journal of cancer.* 2018.

31. Pillay J, Kamp VM, van Hoffen E, Visser T, Tak T, Lammers JW, et al. A subset of neutrophils in human systemic inflammation inhibits T cell responses through Mac-1. *The Journal of clinical investigation.* 2012;122(1):327-36.

32. Mastellos DC, Yancopoulou D, Kokkinos P, Huber-Lang M, Hajishengallis G, Biglarnia AR, et al. Compstatin: a C3-targeted complement inhibitor reaching its prime for bedside intervention. *European journal of clinical investigation.* 2015;45(4):423-40.
33. Lindorfer MA, Cook EM, Reis ES, Ricklin D, Risitano AM, Lambris JD, et al. Compstatin Cp40 blocks hematin-mediated deposition of C3b fragments on erythrocytes: Implications for treatment of malarial anemia. *Clinical immunology.* 2016;171:32-5.
34. Nunn MA, Sharma A, Paesen GC, Adamson S, Lissina O, Willis AC, et al. Complement inhibitor of C5 activation from the soft tick Ornithodoros moubata. *J Immunol.* 2005;174(4):2084-91.
35. Blom AM, Volokhina EB, Fransson V, Stromberg P, Berghard L, Viktorelius M, et al. A novel method for direct measurement of complement convertases activity in human serum. *Clinical and experimental immunology.* 2014;178(1):142-53.
36. Uriarte SM, Rane MJ, Luerman GC, Barati MT, Ward RA, Nauseef WM, et al. Granule exocytosis contributes to priming and activation of the human neutrophil respiratory burst. *J Immunol.* 2011;187(1):391-400.
37. McLeish KR, Uriarte SM, Tandon S, Creed TM, Le J, and Ward RA. Exocytosis of neutrophil granule subsets and activation of prolyl isomerase 1 are required for respiratory burst priming. *Journal of innate immunity.* 2013;5(3):277-89.
38. Lee W, Ko SY, Mohamed MS, Kenny HA, Lengyel E, and Naora H. Neutrophils facilitate ovarian cancer premetastatic niche formation in the omentum. *The Journal of experimental medicine.* 2019;216(1):176-94.
39. Wong JL, Obermajer N, Odunsi K, Edwards RP, and Kalinski P. Synergistic COX2 Induction by IFNgamma and TNFalpha Self-Limits Type-1 Immunity in the Human Tumor Microenvironment. *Cancer immunology research.* 2016;4(4):303-11.

40. Yang L, Zhang X, Ma Y, Zhao X, Li B, and Wang H. Ascites promotes cell migration through the repression of miR-125b in ovarian cancer. *Oncotarget.* 2017;8(31):51008-15.

41. McLane LM, Banerjee PP, Cosma GL, Makedonas G, Wherry EJ, Orange JS, et al. Differential localization of T-bet and Eomes in CD8 T cell memory populations. *J Immunol.* 2013;190(7):3207-15.

42. Matsuzaki J, Tsuji T, Luescher IF, Shiku H, Mineno J, Okamoto S, et al. Direct tumor recognition by a human CD4(+) T-cell subset potently mediates tumor growth inhibition and orchestrates anti-tumor immune responses. *Sci Rep.* 2015;5:14896.

43. Sagiv JY, Michaeli J, Assi S, Mishalian I, Kisos H, Levy L, et al. Phenotypic diversity and plasticity in circulating neutrophil subpopulations in cancer. *Cell reports.* 2015;10(4):562-73.

44. Reis ES, Mastellos DC, Ricklin D, Mantovani A, and Lambris JD. Complement in cancer: untangling an intricate relationship. *Nature reviews Immunology.* 2018;18(1):5-18.

45. Platt JL, Silva I, Balin SJ, Lefferts AR, Farkash E, Ross TM, et al. C3d regulates immune checkpoint blockade and enhances antitumor immunity. *JCI insight.* 2017;2(9).

46. Facciabene A, De Sanctis F, Pierini S, Reis ES, Balint K, Facciponte J, et al. Local endothelial complement activation reverses endothelial quiescence, enabling t-cell homing, and tumor control during t-cell immunotherapy. *Oncoimmunology.* 2017;6(9):e1326442.

47. Cho MS, Vasquez HG, Rupaimoole R, Pradeep S, Wu S, Zand B, et al. Autocrine effects of tumor-derived complement. *Cell reports.* 2014;6(6):1085-95.

48. Cho MS, Rupaimoole R, Choi HJ, Noh K, Chen J, Hu Q, et al. Complement Component 3 Is Regulated by TWIST1 and Mediates Epithelial-Mesenchymal Transition. *J Immunol.* 2016;196(3):1412-8.

773 49. Yuen J, Pluthero FG, Douda DN, Riedl M, Cherry A, Ulanova M, et al. NETosing
774 Neutrophils Activate Complement Both on Their Own NETs and Bacteria via Alternative
775 and Non-alternative Pathways. *Front Immunol.* 2016;7:137.
776 50. Blatt AZ, Saggu G, Cortes C, Herbert AP, Kavanagh D, Ricklin D, et al. Factor H C-
777 Terminal Domains Are Critical for Regulation of Platelet/Granulocyte Aggregate
778 Formation. *Front Immunol.* 2017;8:1586.
779 51. Liu CF, Min XY, Wang N, Wang JX, Ma N, Dong X, et al. Complement Receptor 3 Has
780 Negative Impact on Tumor Surveillance through Suppression of Natural Killer Cell
781 Function. *Front Immunol.* 2017;8:1602.
782 52. Medler TR, Murugan D, Horton W, Kumar S, Cotechini T, Forsyth AM, et al.
783 Complement C5a Fosters Squamous Carcinogenesis and Limits T Cell Response to
784 Chemotherapy. *Cancer cell.* 2018;34(4):561-78 e6.
785 53. Ajona D, Ortiz-Espinosa S, Moreno H, Lozano T, Pajares MJ, Agorreta J, et al. A
786 Combined PD-1/C5a Blockade Synergistically Protects against Lung Cancer Growth and
787 Metastasis. *Cancer discovery.* 2017;7(7):694-703.
788 54. Nunez-Cruz S, Gimotty PA, Guerra MW, Connolly DC, Wu YQ, DeAngelis RA, et al.
789 Genetic and pharmacologic inhibition of complement impairs endothelial cell function
790 and ablates ovarian cancer neovascularization. *Neoplasia.* 2012;14(11):994-1004.
791 55. Lizcano A, Secundino I, Dohrmann S, Corriden R, Rohena C, Diaz S, et al. Erythrocyte
792 sialoglycoproteins engage Siglec-9 on neutrophils to suppress activation. *Blood.*
793 2017;129(23):3100-10.
794 56. Negorev D, Beier UH, Zhang T, Quatromoni JG, Bhojnagarwala P, Albelda SM, et al.
795 Human neutrophils can mimic myeloid-derived suppressor cells (PMN-MDSC) and
796 suppress microbead or lectin-induced T cell proliferation through artefactual
797 mechanisms. *Sci Rep.* 2018;8(1):3135.

57. Singel KL, and Segal BH. Neutrophils in the tumor microenvironment: trying to heal the wound that cannot heal. *Immunological reviews.* 2016;273(1):329-43.
58. Coffelt SB, Kersten K, Doornebal CW, Weiden J, Vrijland K, Hau CS, et al. IL-17-producing gammadelta T cells and neutrophils conspire to promote breast cancer metastasis. *Nature.* 2015;522(7556):345-8.
59. Wculek SK, and Malanchi I. Neutrophils support lung colonization of metastasis-initiating breast cancer cells. *Nature.* 2015;528(7582):413-7.
60. Steele CW, Karim SA, Leach JDG, Bailey P, Upstill-Goddard R, Rishi L, et al. CXCR2 Inhibition Profoundly Suppresses Metastases and Augments Immunotherapy in Pancreatic Ductal Adenocarcinoma. *Cancer cell.* 2016;29(6):832-45.
61. Nywening TM, Belt BA, Cullinan DR, Panni RZ, Han BJ, Sanford DE, et al. Targeting both tumour-associated CXCR2(+) neutrophils and CCR2(+) macrophages disrupts myeloid recruitment and improves chemotherapeutic responses in pancreatic ductal adenocarcinoma. *Gut.* 2018;67(6):1112-23.
62. Clark RA, and Klebanoff SJ. Neutrophil-mediated tumor cell cytotoxicity: role of the peroxidase system. *The Journal of experimental medicine.* 1975;141(6):1442-7.
63. Eruslanov EB, Bhojnagarwala PS, Quatromoni JG, Stephen TL, Ranganathan A, Deshpande C, et al. Tumor-associated neutrophils stimulate T cell responses in early-stage human lung cancer. *The Journal of clinical investigation.* 2014;124(12):5466-80.
64. Futosi K, and Mocsai A. Tyrosine kinase signaling pathways in neutrophils. *Immunological reviews.* 2016;273(1):121-39.
65. Lofgren R, Serrander L, Forsberg M, Wilsson A, Wasteson A, and Stendahl O. CR3, FcgammaRIIA and FcgammaRIIIB induce activation of the respiratory burst in human neutrophils: the role of intracellular Ca(2+), phospholipase D and tyrosine phosphorylation. *Biochimica et biophysica acta.* 1999;1452(1):46-59.

66. Forsberg M, Lofgren R, Zheng L, and Stendahl O. Tumour necrosis factor-alpha potentiates CR3-induced respiratory burst by activating p38 MAP kinase in human neutrophils. *Immunology.* 2001;103(4):465-72.
67. Nagaraj S, Gupta K, Pisarev V, Kinarsky L, Sherman S, Kang L, et al. Altered recognition of antigen is a mechanism of CD8+ T cell tolerance in cancer. *Nature medicine.* 2007;13(7):828-35.
68. Corzo CA, Cotter MJ, Cheng P, Cheng F, Kusmartsev S, Sotomayor E, et al. Mechanism regulating reactive oxygen species in tumor-induced myeloid-derived suppressor cells. *J Immunol.* 2009;182(9):5693-701.
69. Michaeli J, Shaul ME, Mishalian I, Hovav AH, Levy L, Zolotriov L, et al. Tumor-associated neutrophils induce apoptosis of non-activated CD8 T-cells in a TNFalpha and NO-dependent mechanism, promoting a tumor-supportive environment. *Oncoimmunology.* 2017;6(11):e1356965.
70. Gao R, Ma J, Wen Z, Yang P, Zhao J, Xue M, et al. Tumor cell-released autophagosomes (TRAP) enhance apoptosis and immunosuppressive functions of neutrophils. *Oncoimmunology.* 2018;7(6):e1438108.
71. Grassi L, Pourfarzad F, Ullrich S, Merkel A, Were F, Carrillo-de-Santa-Pau E, et al. Dynamics of Transcription Regulation in Human Bone Marrow Myeloid Differentiation to Mature Blood Neutrophils. *Cell reports.* 2018;24(10):2784-94.
72. Bjerregaard MD, Jurlander J, Klausen P, Borregaard N, and Cowland JB. The in vivo profile of transcription factors during neutrophil differentiation in human bone marrow. *Blood.* 2003;101(11):4322-32.
73. Lindemann SW, Yost CC, Denis MM, McIntyre TM, Weyrich AS, and Zimmerman GA. Neutrophils alter the inflammatory milieu by signal-dependent translation of constitutive messenger RNAs. *Proceedings of the National Academy of Sciences of the United States of America.* 2004;101(18):7076-81.

74. Federzoni EA, Valk PJ, Torbett BE, Haferlach T, Lowenberg B, Fey MF, et al. PU.1 is linking the glycolytic enzyme HK3 in neutrophil differentiation and survival of APL cells. *Blood.* 2012;119(21):4963-70.

75. Predina J, Eruslanov E, Judy B, Kapoor V, Cheng G, Wang LC, et al. Changes in the local tumor microenvironment in recurrent cancers may explain the failure of vaccines after surgery. *Proceedings of the National Academy of Sciences of the United States of America.* 2013;110(5):E415-24.

76. Joseph N, Clark RM, Dizon DS, Lee MS, Goodman A, Boruta D, Jr., et al. Delay in chemotherapy administration impacts survival in elderly patients with epithelial ovarian cancer. *Gynecologic oncology.* 2015;137(3):401-5.

77. Singh S, Guetzko M, and Resnick K. Preoperative predictors of delay in initiation of adjuvant chemotherapy in patients undergoing primary debulking surgery for ovarian cancer. *Gynecologic oncology.* 2016;143(2):241-5.

78. Janols H, Bergenfelz C, Allaoui R, Larsson AM, Ryden L, Bjornsson S, et al. A high frequency of MDSCs in sepsis patients, with the granulocytic subtype dominating in gram-positive cases. *J Leukoc Biol.* 2014;96(5):685-93.

79. Kolomeyevskaya N, Eng KH, Khan AN, Grzankowski KS, Singel KL, Moysich K, et al. Cytokine profiling of ascites at primary surgery identifies an interaction of tumor necrosis factor-alpha and interleukin-6 in predicting reduced progression-free survival in epithelial ovarian cancer. *Gynecologic oncology.* 2015;138(2):352-7.

80. Gustafson MP, Lin Y, Maas ML, Van Keulen VP, Johnston PB, Peikert T, et al. A method for identification and analysis of non-overlapping myeloid immunophenotypes in humans. *PloS one.* 2015;10(3):e0121546.

Figures and Legends

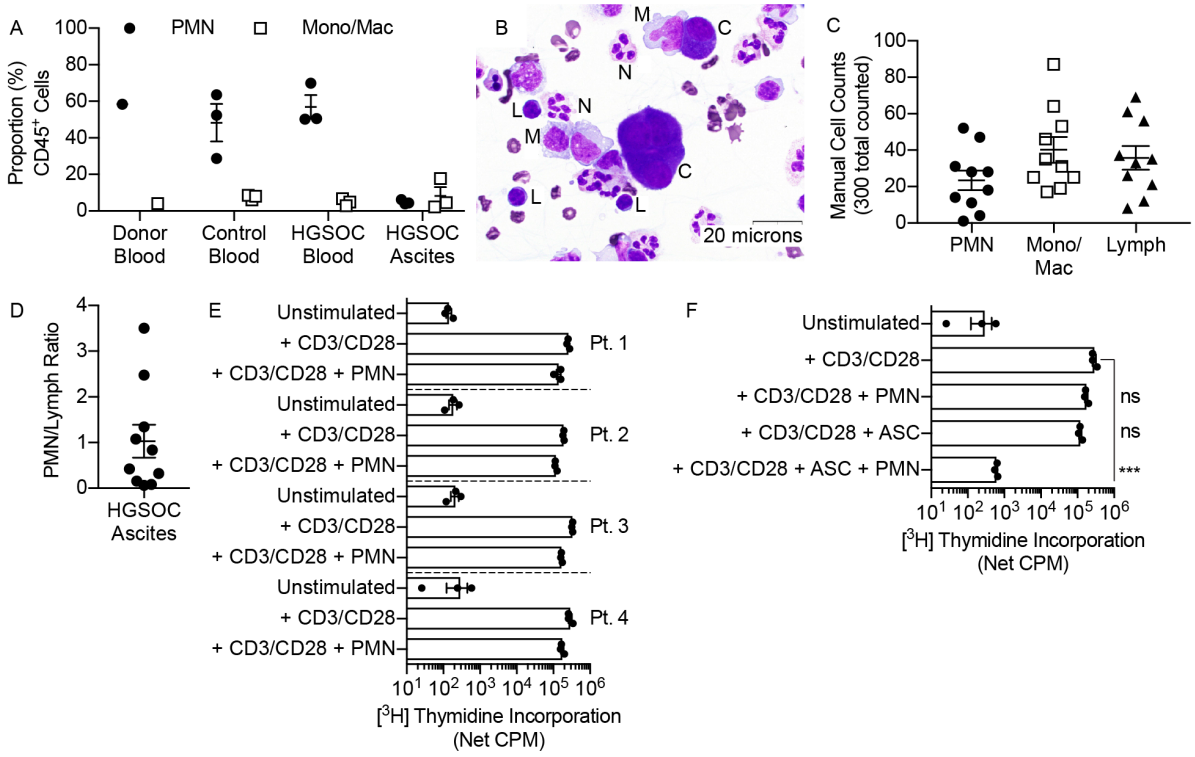

Figure 1. Ovarian cancer ascites induces circulating patient PMN to become suppressive. A) The proportion of circulating WBC populations in a healthy donor (n=1), control female patients undergoing surgery for a benign peritoneal mass (n=3), and patients undergoing surgery for newly diagnosed HGSOC (n=3) are similar, but differ significantly from WBC populations in paired HGSOC ascites (n=3). B-D) Cytologic analysis of Wright Giemsa-stained cytospins of ascites from newly diagnosed HGSOC (n=10). B) Representative image showing mature PMN (N), monocytes/macrophages (M), lymphocytes (L), and tumor cells (C). All PMN were morphologically mature with characteristic segmented nuclei. C) WBC proportions were quantified: PMN 4-52%, monocytes/macrophage 17-87%, and lymphocytes 8-69%. D) Mean PMN-to-lymphocyte ratio was 1.03 [95% CI 0.21-1.8, SEM 0.4]. E-F) T cells ($CD3^+$) and PMN were isolated from patient blood and used in autologous coculture at 1:1 based on data in (D) (n=4). PMN and/or ascites supernatants (ASC; 50% final well volume) were added to anti-CD3/CD28-stimulated T cells. After 72h of coculture, T cell proliferation was measured by [^{3}H] thymidine incorporation (16-18h). E) HGSOC patient circulating PMN were negligibly T cell suppressive. F) ASC are not suppressive alone but induce patient PMN to suppress stimulated T cell proliferation by a factor of 2.08 $\log_{10}$ [95% CI 1.26-2.90]. Symbols represent individual samples (n) and bars represent SEM. Statistical comparisons were by ANOVA with Tukey post-test, *(*, p<0.05; **, p<0.01; ***, p<0.001; ns, not significant)*.

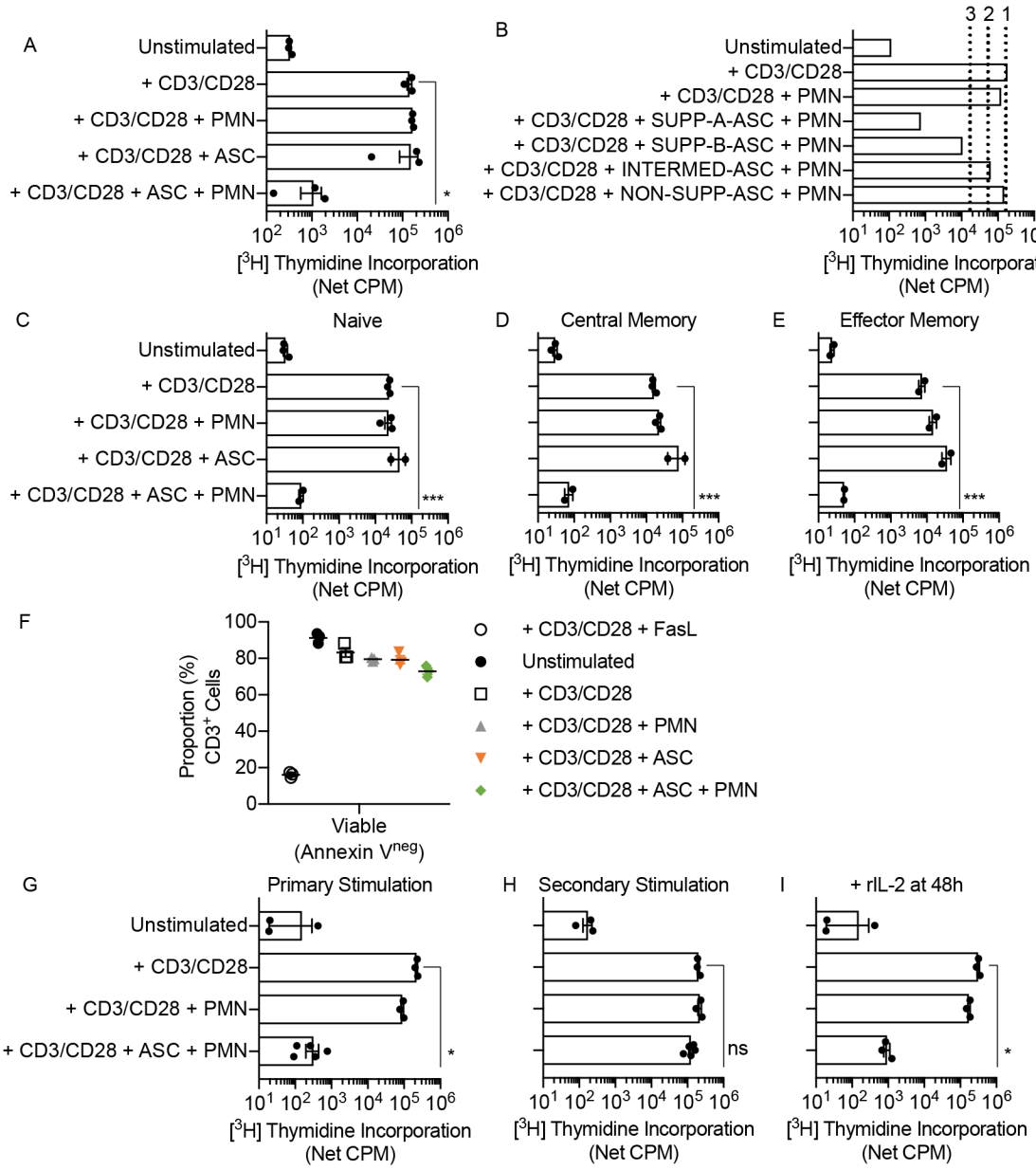

893

894 **Figure 2. Suppressed T cells are viable and responsive to secondary stimulation.** T cells
895 ($CD3^+$) and PMN were used in autologous coculture at 1:1. PMN and/or ascites supernatants
896 (ASC; 50% final well volume) were added to anti-CD3/CD28-stimulated T cells. After 72h of
897 coculture, T cell proliferation was measured by [^{3}H] thymidine incorporation (16-18h). A) Results
898 are consistent with soluble anti-CD3/CD28 Ab or anti-CD3/CD28 microbeads as T cell stimulus.
899 B) ASC (n=31) were stratified into three categories based on the induction of a PMN suppressor
900 phenotype, where x equals a reduction in proliferation as compared to anti-CD3/CD28-
901 stimulated T cells alone: suppressors (SUPP, line 3; $x \geq 1$ $\log_{10}$), intermediate suppressors
902 (INTERMED, line 2; 0.5 $\log_{10} \leq x < 1$ $\log_{10}$), and non-suppressors (NON-SUPP, line 1; $x < 0.5$
903 $\log_{10}$). SUPP-A and B illustrate that a subset of ascites supernatants induced PMN suppressors
904 $x \geq 2$ $\log_{10}$. Bars are representative. C-E) PMN suppressor phenotype fully suppressed anti-
905 CD3/CD28-stimulated C) naïve ($CD3^+CD45RA^+RO^{neg}CD62L^+$), D) central memory

(CD3$^+$CD45RA^{neg}RO$^+$CD62L$^+$), and E) effector memory (CD3$^+$CD45RA^{neg}RO$^+$CD62L^{neg}) T cell populations (n=2). F) T cells were annexin-V negative (≥70%) after 72h coculture with ASC (n=3) and/or PMN. Fas ligand was added to stimulated T cells as a positive control for apoptosis. G) Stimulated T cell proliferation was suppressed after 72h with ASC and PMN, but H) restored after ASC removal and anti-CD3/CD28-restimulation (n=5). I) Addition of rIL-2 (100 IU) at 48h did not rescue T cell proliferation, as assessed at 72h. Symbols represent individual samples (n) and bars represent SEM. Statistical comparisons were by ANOVA with Tukey post-test *(*, p<0.05; **, p<0.01; ***, p<0.001; ns, not significant).* Results were consistent between CD4$^+$ and CD8$^+$ T cells.

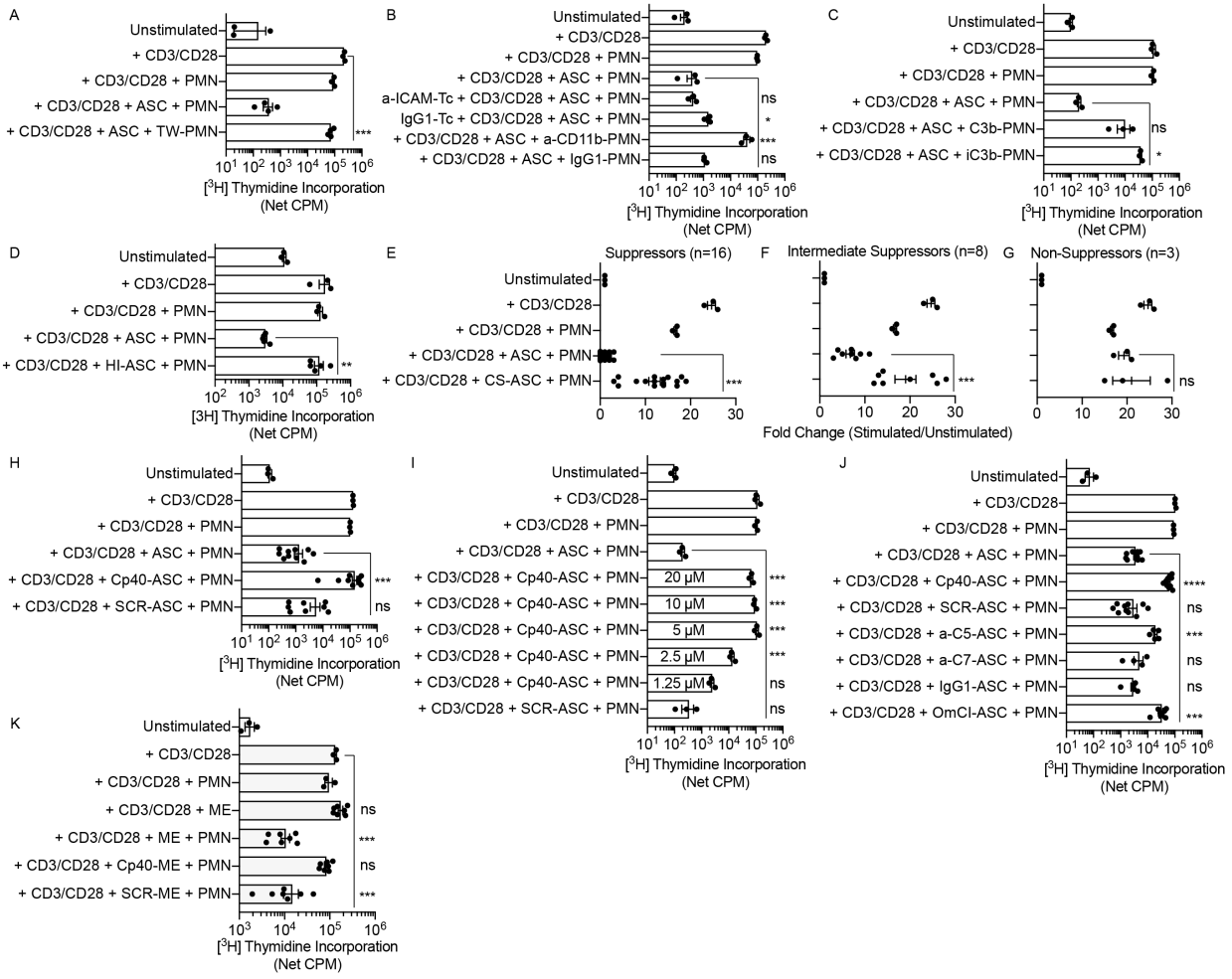

Figure 3. PMN suppressor phenotype requires contact between PMN and T cells, complement C3 activation, and complement receptor 3. T cells ($CD3^+$) and PMN were used in autologous coculture at 1:1. PMN and/or ascites supernatants (ASC; 50% final well volume) were added to anti-CD3/CD28-stimulated T cells. After 72h of coculture, T cell proliferation was measured by [^{3}H] thymidine incorporation (16-18h). A) T cells were stimulated with anti-CD3/CD28 in the bottom chamber. PMN and ASC added to the transwell insert did not suppress T cell proliferation, suggesting that suppression is contact-dependent (n=4). B) T cells treated with anti-ICAM-1 Ab (1-10 µg) for 1h prior to coculture had no effect on proliferation. PMN treated with anti-CD11b Ab for 1h prior to coculture abrogated the suppressor phenotype. Treatment of T cells or PMN with IgG1 isotype (1-10 µg) had no effect on proliferation (n=5). C) PMN pretreated with C3b or iC3b (40-160 µg/mL) prior to coculture were unable to induce the PMN suppressor phenotype. D) ASC were heat-inactivated (HI-ASC; 56°C, 1h) prior to coculture and abrogated the PMN suppressor phenotype (n=5). E-H) Two formulations of compstatin, CS and Cp40, were used to inhibit C3 activation. E-G) Addition of CS (250 µM) to ASC (CS-ASC) 2h prior to coculture with PMN and T cells abrogated the PMN suppressor phenotype (n=27). H) Addition of Cp40 (20 µM) to ASC (Cp40-ASC) 2h prior to coculture also abrogated the PMN suppressor phenotype, while scramble peptide (SCR-ASC, 20 µM) had no effect (n=10). I) A titration study showed that 5 µM Cp40 was sufficient to fully abrogate the PMN suppressor phenotype (n=3). J) ASC were pretreated with neutralizing Ab anti-C5 or C7,

935 or with OmCI, a peptide inhibitor of C5, prior to coculture. Anti-C5 and OmCI partially abrogated
936 the PMN suppressor phenotype, as compared to their respective controls, whereas anti-C7 did
937 not affect the suppressor phenotype. K) Malignant effusions (ME), including pelural fluid and
938 ascites from patients with a number of metastatic cancers induced the PMN suppressor
939 phenotype, which was abrogated by Cp40-treatment in all of the tested samples (n=7; see
940 Table 3). Symbols represent individual samples (n) and bars represent SEM. Statistical
941 comparisons were by ANOVA with Tukey post-test or by Mann-Whitney *(*, p<0.05; **, p<0.01;*
942 ****, p<0.001; ns, not significant).*

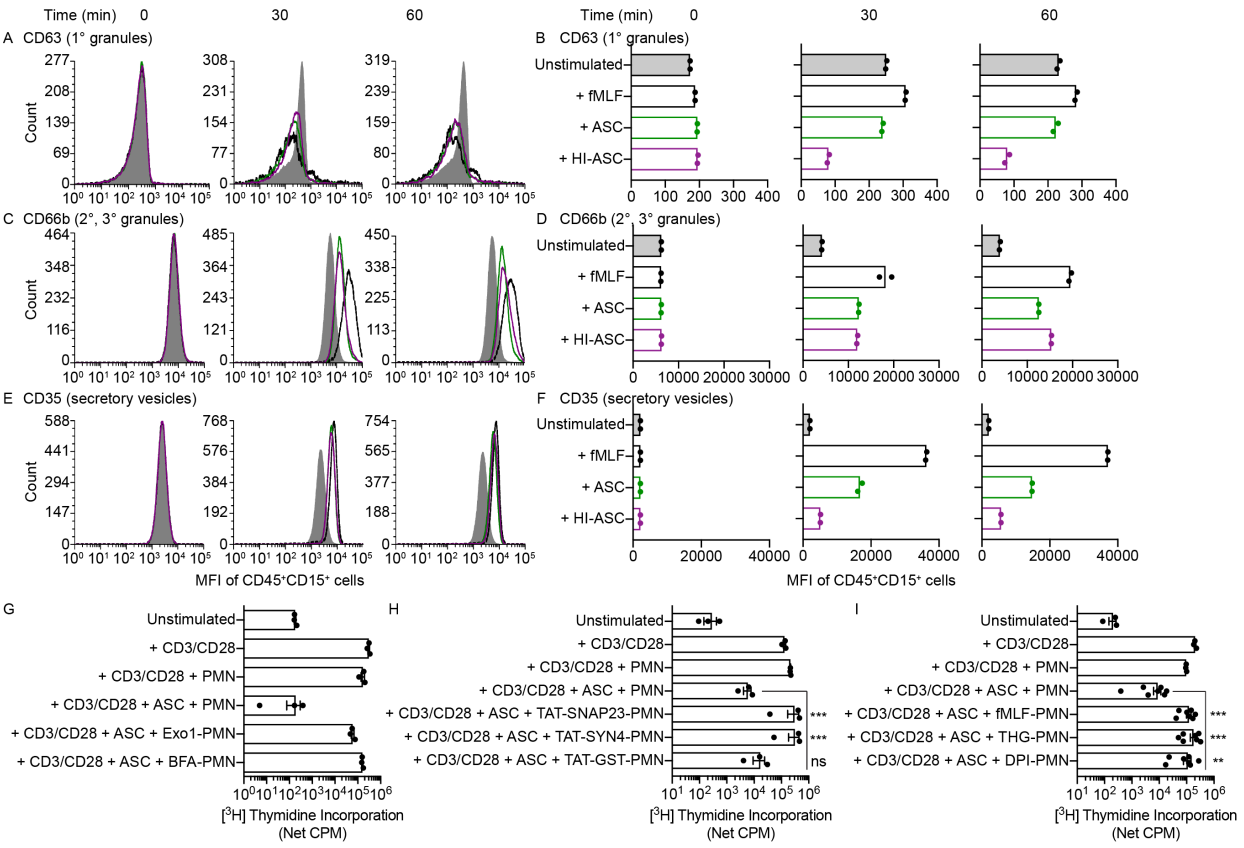

943

944 **Figure 4. PMN suppressor phenotype requires SNARE transport and Ca^{2+} mobilization,**
945 **and is abrogated by desensitization with fMLF.** A-F) PMN were treated with media, fMLF
946 (100 nM), ASC (n=3), or heat-inactivated ASC (HI-ASC; n=3) and assessed for markers of
947 membrane fusion with primary (CD63), secondary and tertiary (CD66b) granules, and secretory
948 vesicles (CD35) at 0, 30, and 60 min. PMN were gated on $CD45^+CD15^+$. A, C, E) The MFI
949 overlays are representative; unstimulated PMN in media, grey solid; fMLF, black dashed line;
950 ASC, green line; HI-ASC, purple line. B, D, F) MFI quantification. G-I) T cells ($CD3^+$) and PMN
951 were used in autologous coculture at 1:1. PMN and/or ascites supernatants (ASC; 50% final
952 well volume) were added to anti-CD3/CD28-stimulated T cells. After 72h of coculture, T cell
953 proliferation was measured by $[^3H]$ thymidine incorporation (16-18h). G) Pretreatment with
954 brefeldin-A (BFA; 1-10 µg/mL) or ER export inhibitor 1 (Exo1; 20-75 µM) abrogated the
955 suppressor phenotype, indicating a requirement for exocytosis (n=3). H) PMN pretreated with
956 TAT-SNAP23 (0.6 µg) or TAT-SYN4 (0.6 µg) abrogated the PMN suppressor phenotype. TAT-
957 GST (0.6 µg) used as a specificity control had no effect (n=3). I) PMN pretreated with fMLF (100
958 nM), thapsigargin (THG, 1 µM), or diphenyleneiodonium (DPI, 1 µM) abrogated the PMN
959 suppressor phenotype (n=7). Symbols represent individual samples (n) and bars represent
960 SEM. Statistical comparisons were by ANOVA with Tukey post-test *(*, p<0.05; **, p<0.01; ***,*
961 *p<0.001; ns, not significant).*

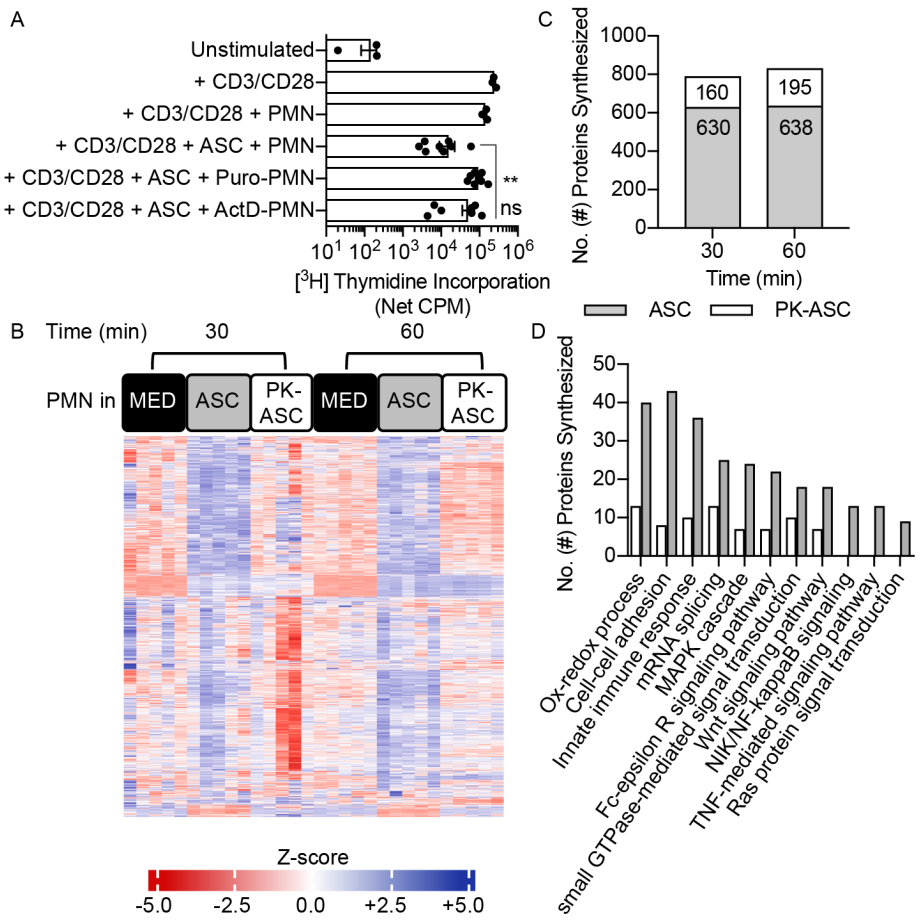

962

963 **Figure 5. Ascites induces robust *de novo* protein synthesis in PMN, which is required for**
964 **the suppressor phenotype.** A) PMN pretreated with puromycin (1 µg) for 1h prior to coculture
965 abrogated the PMN suppressor phenotype, while D-actinomycin (1 µg) pretreatment had more
966 variable effects (n=8). B-D) PMN were exposed to media, ASC, or proteinase K-digested ASC
967 (PK-ASC) for 30 or 60 min in 5 replicates per condition per time point. PMN were washed and
968 frozen as dry pellets for proteomics analysis. B) Heat-map showing that the protein profiles of
969 PMN exposed to ASC have higher Z-scores than either PMN exposed to media or PK-ASC at
970 30 and 60 min. C) The number of changed proteins (y-axis) in PMN exposed to ASC is
971 significantly greater than in PMN exposed to PK-ASC (*p=0.02*); there was no significant
972 difference between 30 or 60 min. D) Gene ontology analysis shows that ASC induced new
973 synthesis of multiple classes of proteins in PMN. Symbols represent individual samples (n) and
974 bars represent SEM. Statistical comparisons were by ANOVA with Tukey post-test *(*, p<0.05;*
975 ***, p<0.01; ***, p<0.001; ns, not significant).*

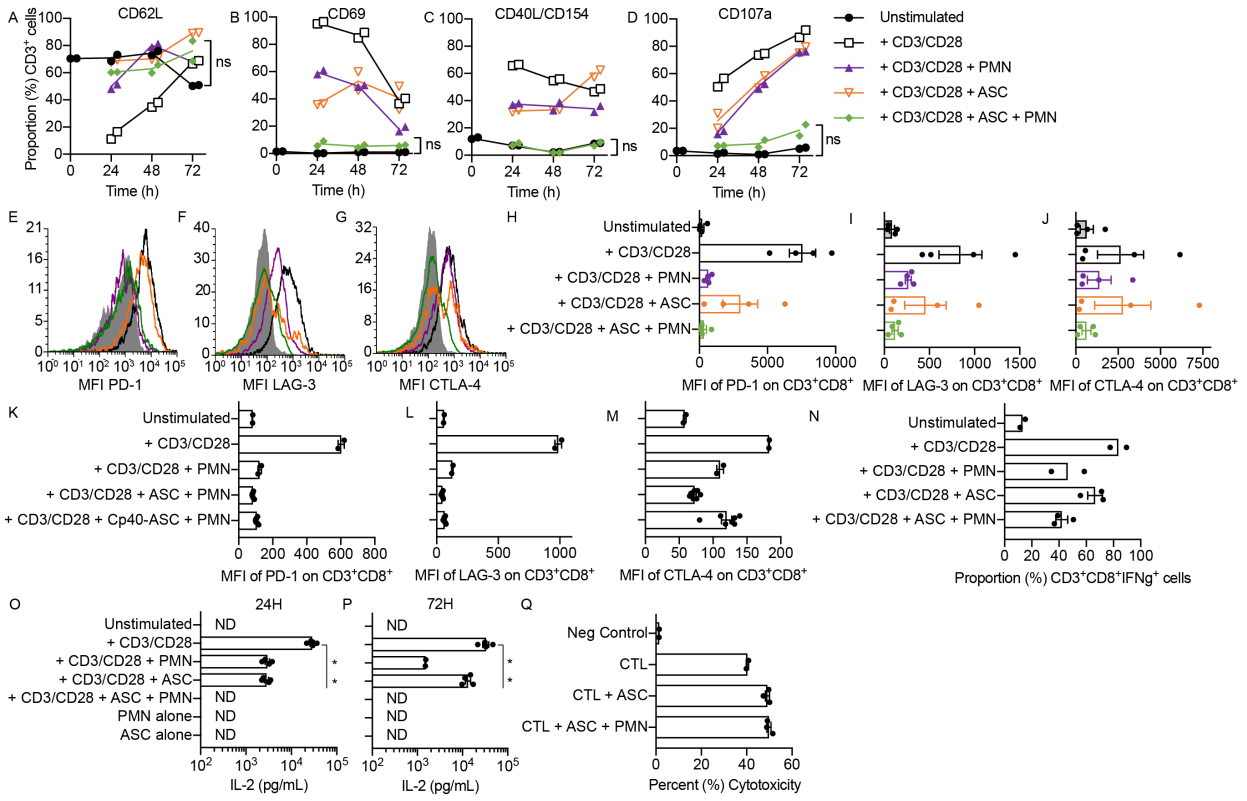

Figure 6. Combination of ascites and PMN prevents T cell activation and is independent of exhaustion. T cells ($CD3^+$) and PMN were used in autologous coculture at 1:1. PMN and/or ascites supernatants (ASC; 50% final well volume) were added to anti-CD3/CD28-stimulated T cells. At 24, 48, and 72h, T cells were analyzed for surface and intracellular expression of markers for activation, co-stimulation, and function. Surface expression of A) CD62L, B) CD69, C) CD40L, and D) CD107a were evaluated at baseline (on y-axis) and at 24, 48, and 72h (n=2). E-M) PD-1, LAG-3, and CTLA-4 expression was evaluated (n=4). $CD8^+$ T cells at 72h are represented here in representative MFI overlays (E-G) and quantification (H-J); unstimulated T cells in media, grey solid; anti-CD3/CD28-stimulated, black dashed line; anti-CD3/CD28-stimulated + PMN, purple solid line; anti-CD3/CD28-stimulated + ASC, orange solid line; anti-CD3/CD28-stimulated + ASC + PMN, green solid line. K-M) Stimulated T cell expression of PD-1 and LAG-3 after coculture with Cp40-ASC and PMN was unaffected as compared to unstimulated, but CTLA-4 showed an upwards trend (n=6). N) At 72h, intracellular expression of IFN-gamma was reduced as compared to stimulated alone (n=3). O-P) Combination of ASC and PMN reduced anti-CD3/CD28-stimulated T cell IL-2 levels (pg/mL) in supernatants to ND after 24 (O) and 72h (P) of coculture (n=4). Background levels of PMN or ASC were ND; ND=non-detectable. Q) CTL activity of NY-ESO-$1_{157-165}$-specific $CD8^+$ T cells directed at SK29 target cells pulsed with the NY-ESO-1 peptide was unaffected by coculture with ASC and/or PMN (n=3). Symbols represent individual samples (n) and bars represent SEM. Statistical comparisons were by Mann-Whitney *(*, p<0.05; **, p<0.01; ***, p<0.001; ns, not significant).* Results were consistent between $CD4^+$ and $CD8^+$ T cells.

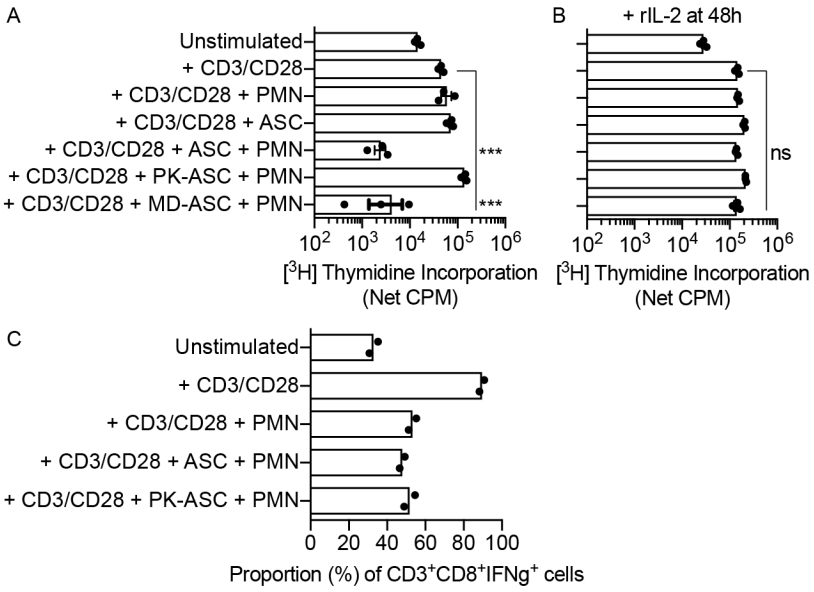

998

999 **Figure 7. PMN suppressor phenotype inhibits engineered effector T cell activation but**
1000 **not antigen-specific cytotoxicity.** Engineered CTL expressing NYESO1-specific TCR (TCR-
1001 CTL) are candidates for adoptive cell therapy in EOC. TCR-CTL and PMN were used in
1002 coculture at 1:1. PMN and/or ascites supernatants (ASC; 50% final well volume) were added to
1003 anti-CD3/CD28-stimulated TCR-CTL. After 72h of coculture (A) or after rIL-2 (100 IU) addition at
1004 48h (B), CTL proliferation was measured by [^{3}H] thymidine incorporation (16-18h) (n=3). A) ASC
1005 and MD-ASC rendered PMN suppressive to TCR-CTL, while PK-ASC had no effect. B) Addition
1006 of rIL-2 reversed suppression. C) IFN-gamma expression was reduced with PMN and/or ASC or
1007 PK-ASC, as measured by flow cytometry after 72h of coculture (n=2). Symbols represent
1008 individual samples (n) and bars represent SEM. Statistical comparisons were by ANOVA with
1009 Tukey post-test *(*, p<0.05; **, p<0.01; ***, p<0.001; ns, not significant).*

	Suppressor Status			
	Suppressor ($x \geq 1 \log_{10}$)	Intermediate ($0.5 \log_{10} \leq x < 1 \log_{10}$)	Non ($x < 0.5 \log_{10}$)	p-value
N (31)	20	8	3	
Pre-operative CBC	16/20	7/8	3/3	
WBC (x10^9 cells/L)	8.6	8.5	9.3	0.94
% HCT	36.1	35.6	39.6	0.62
PLT (x10^9 cells/L)	411.0	565.0	352.3	0.22
Differential	13/20	6/8	3/3	
PMN (x10^9 cells/L)	6.3	6.5	6.1	0.93
Lymphocyte (x10^9 cells/L)	1.3	1.2	2.2	0.56
Monocyte (x10^9 cells/L)	0.6	0.5	0.7	0.71
NLR	4.7	5.5	2.8	0.73
Manual Counts	7/20	3/8	1/3	
% Segmented PMN	67.0	77.5	73.2	0.30
% Bands	1.0	NR	NR	
% Metamyelocytes	NR	NR	NR	

Table 1. Patients with newly diagnosed EOC have normal circulating WBC numbers and differentials. Data are based on review of electronic health records at Roswell Park Comprehensive Cancer Center. Statistical comparisons were by ANOVA with Tukey post-test. CBC, complete blood cell count; WBC, white blood cell; HCT, hematocrit; PLT, platelet; NLR, neutrophil-to-lymphocyte ratio; NR, none recorded.

	Suppressor Status			
	Suppressor ($x \geq 1$ $\log_{10}$)	Intermediate (0.5 $\log_{10} \leq x < 1$ $\log_{10}$)	Non ($x < 0.5$ $\log_{10}$)	p-value
N (31)	20	8	3	
Age, Mean	65.4	69.6	64.0	0.39
Histology				0.40
EOC, serous	15	6	2	
EOC, non-serous	2	0	0	
OC, non-epithelial	3	2	0	
Benign, thecoma	0	0	1	
Stage				0.62
IIIA	1	0	0	
IIIB	1	1	0	
IIIC	16	6	2	
IV	2	1	0	
Grade 3	19	8	2	1.00
CA125	576.7 (n=12)	360.5 (n=5)	9251.1 (n=1)	0.44
Debulking Surgery	15/20	6/8	1/3	
% R0	46.7	16.7	0	0.14
% Optimal	40.0	50.0	100.0	0.57
% Suboptimal	13.3	33.3	0	0.44
Chemotherapy Response*	12/20	2/8	1/3	
% Platinum Sensitive	75.0	100.0	100.0	0.58
% Platinum Resistant	16.7	0	0	0.44
% Platinum Refractory	8.3	0	0	0.60
*: RECiST Evaluation complete response after end of adjuvant chemotherapy				

Table 2. Ascites stratification strategy based on the induction of a suppressor phenotype in PMN. Ascites were stratified into three categories based on the induction of a suppressor phenotype in PMN, where x equals a reduction in proliferation as compared to anti-CD3/CD28-stimulated T cells alone: suppressors ($x \geq 1$ $\log_{10}$), intermediate suppressors (0.5 $\log_{10} \leq x < 1$ $\log_{10}$), and non-suppressors ($x < 0.5$ $\log_{10}$). Statistical comparisons were by ANOVA with Tukey post-test.

Demographics of Patients with Malignant Effusions other than EOC Ascites	
N	7
Age, Mean (Y)	68.4
Sex (Female:Male)	5:2
Type of Malignant Effusions	
Peritoneal Ascites	1
Pleural Effusion	6
Metastatic Cancer	
Ovarian	2
Lung	2
Pancreatic*	1
GI	1
Lymphoma	1
Newly Diagnosed	3
Received Prior Treatment (e.g., surgery, chemotherapy, immunotherapy)	4

*Ascites

Table 3. Clinical characteristics of patients with malignant effusions that induced the PMN suppressor phenotype in a complement C3-dependent mechanism.